GEOPHYSICAL STUDIES OF THE ACKLEY INTRUSIVE SUITE AND THE NORTHEASTERN GANDER ZONE, NEWFOUNDLAND

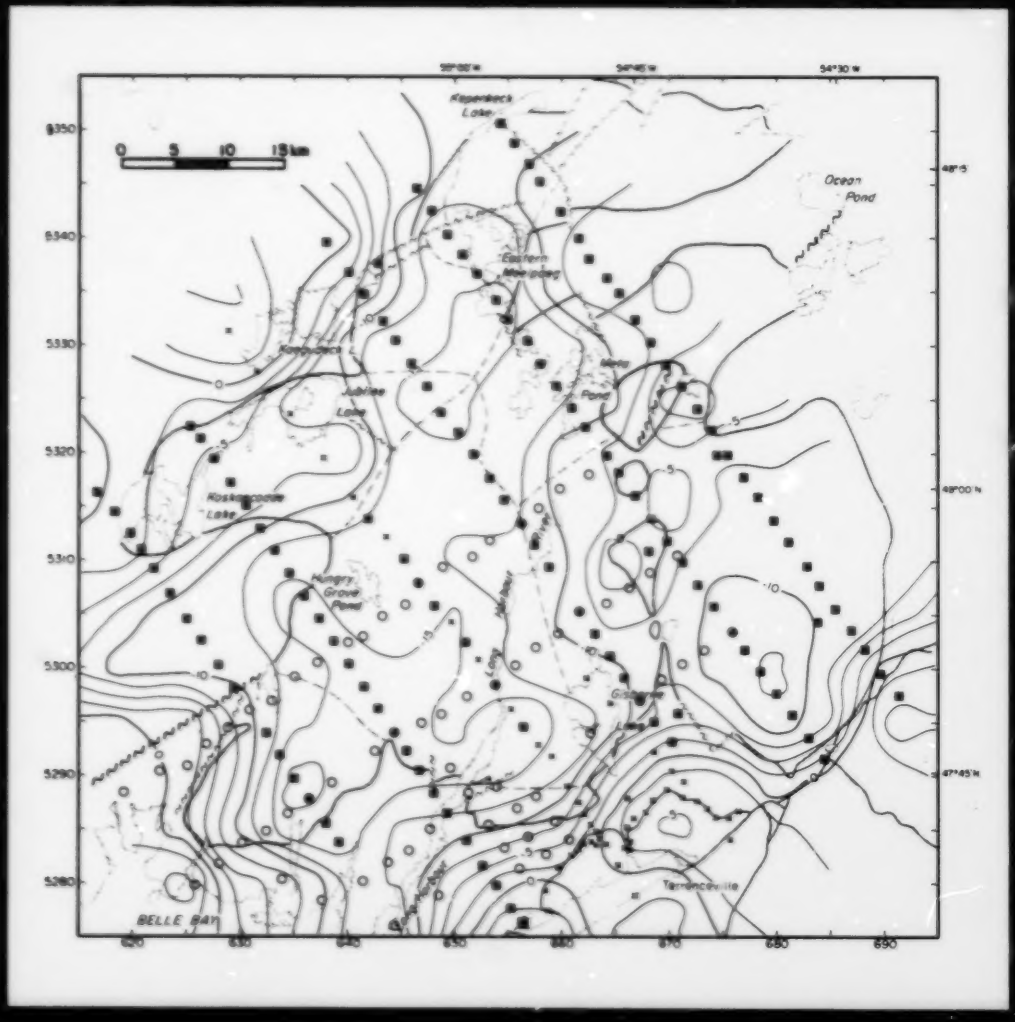

91-02821/

Cover

Bouguer anomaly map for the Ackley intrusive suite area.

GEOLOGICAL SURVEY OF NEWFOUNDLAND
DEPARTMENT OF MINES
GOVERNMENT OF NEWFOUNDLAND AND LABRADOR

GEOPHYSICAL STUDIES OF THE ACKLEY INTRUSIVE SUITE AND THE NORTHEASTERN GANDER ZONE, NEWFOUNDLAND

Hugh G. Miller

Report 88-3

St. John's, Newfoundland
1988

Author's Address *HUGH MILLER*
Department of Earth Sciences
Centre for Earth Resources Research
Memorial University of Newfoundland
St. John's, Newfoundland
Canada
A1B 3X5

EDITING, LAYOUT AND DRAFTING

Senior Geologist R.F. BLACKWOOD

Editor C.P.G. PEREIRA

Copy Editor D. WALSH

Typesetting B. STRICKLAND

Word Processing K. CONNORS
D. DOWNEY
J. MATTHEWS
D. PEAVY
B. STRICKLAND

Supervisor, Cartographic and Photomechanical Services K. BYRNE

Cartography D. LEONARD (Photomechanical)
G. DENIEF
T. PALTANAVAGE
T. SEARS

Publications of the Geological Survey of Newfoundland are available through the Publications and Information Section, Geological Survey of Newfoundland, Department of Mines, P.O. Box 4750, St. John's, Newfoundland, A1C 5T7.
Telephone: (709) 576-3159
Telex: 016-4724
Fax: (709) 576-3493

This project is a contribution to the Canada–Newfoundland Mineral Development Subsidiary Agreement 1984-1989. Project carried out by Newfoundland Department of Mines.

ISBN–0-920769-43-8

TABLE OF CONTENTS

	Page
ABSTRACT	xi
INTRODUCTION	i
GEOPHYSICAL AND GEOCHEMICAL INTERPRETATION OF THE ACKLEY INTRUSIVE SUITE AND ADJOINING COUNTRY ROCKS	
INTRODUCTION	1
OBJECTIVES	1
GEOLOGY AND GEOCHEMISTRY REVIEW	1
GEOPHYSICS REVIEW	1
QUALITATIVE GEOPHYSICAL INTERPRETATION	1
Gravity	2
Survey and Data Reduction	2
Physical Properties	2
Analysis	4
Magnetics	4
Techniques	6
Analysis	6
QUANTITATIVE GEOPHYSICAL INTERPRETATION	7
2½-D Inversion	9
Technique	9
Analysis	10
3-D Inversion	10
Technique	10
Magnetic Modelling	10
COMBINED GEOPHYSICAL AND GEOCHEMICAL INTERPRETATION	13
Technique	13
Analysis	13
Gravity–Density Correlation	15
Silica–Density and Silica–Gravity Correlations	15
Other Geochemical–Density Correlations	16
SUMMARY	17
CONCLUSIONS	18
THE NORTHEASTERN GANDER ZONE	18
INTRODUCTION	18
GEOLOGICAL REVIEW	18
GEOPHYSICAL REVIEW	18
PRESENT STUDY	21
QUALITATIVE INTERPRETATION	21
QUANTITATIVE INTERPRETATION	22
SUMMARY	29
CONCLUSIONS	30
GENERAL CONCLUSIONS	32
ACKNOWLEDGMENTS	32
REFERENCES	32
APPENDIX 1–Gravity Data Acquisition and Reduction	33
APPENDIX 2–Magnetic Data Reduction	37
	39

Page

APPENDIX 3–3-D Gravity Inversion..... 40

APPENDIX 4–Spatial Cross-correlation Techniques..... 42

APPENDIX 5–Reduced Bouguer Anomaly Data..... 43

LIST OF FIGURES

Page

Figure 1: Map showing Newfoundland and location of the two study sites: (1) the Ackley intrusive suite, and (2) the northeastern Gander Zone..... 1

Figure 2: Simplified geological map of Ackley intrusive suite and surrounding rocks; the nomenclature is from Tuach (1987); coordinates are UTM Zone 21. and in kilometres; map scale 1:250,000; same coordinates and scale used in Figures 3 to 10 and 12 to 14; *solid line*, external boundary of Ackley intrusive suite with country rocks; *dashed line*, internal boundaries of Ackley intrusive suite..... 2

Figure 3: Bouguer anomaly map for the Ackley study area; contour interval 2.5 mGal; X, stations from 1983 survey; ⊞ stations from 1985 survey; ○, stations from 1986 survey; geological map and coordinates same as Figure 2..... 3

Figure 4: Density contrast map for the Ackley study area; density contrast = rock density minus 2.67 g cm^{-3}; contour interval 0.05 g cm^{-3}..... 5

Figure 5: Total-field magnetic anomaly map for the Ackley study area based on 4 km filtered data (technique discussed in Appendix 2); contour interval 50 nT; AB, interpreted profile..... 7

Figure 6: Magnetic susceptibility map for the Ackley study area; contours drawn at 0.25, 0.5, 1.0, 2.0, 4.0 cgs susceptibility units..... 8

Figure 7: Second-derivative magnetic map for the Ackley study area; contour interval 10 nT/km^2..... 9

Figure 8: Granite thickness map from 2½-D inversion for the Ackley study area; contour interval 1.0 km..... 11

Figure 9: Granite thickness for the Ackley study area from 3-D inversion method with variable density; contour interval 1.0 km..... 12

Figure 10: Granite thickness for the Ackley study area from 3-D inversion method with constant density; contour interval 1.0 km..... 14

Figure 11: Magnetic model for profile AB on Figure 5; X, observed filtered data; •, data calculated from model; VV Avalon Roof Pendants, + granitic rocks; geological boundaries shown; *solid line*, magnetic body; *dashed line*, bottom of granite from Figure 10..... 15

Figure 12: Gravity–density correlation map for the Ackley study area; contour interval 0.25..... 16

Figure 13: Silica–gravity correlation map for the Ackley study area; contour interval 0.25..... 17

Figure 14: Parallel lineament features in the Ackley study area..... 19

Figure 15: General geology of northeastern Gander Zone based on Andrews (1980), Blackwood *et al.* (1983) and Blackwood (1981a, b); coordinates are UTM Zone 21, and in kilometres; map scale 1:250,000; same coordinates and scale used in Figures 16 to 22. ~ Square Pond Gneiss, Hare Bay Gneiss; + various granites; *blank area*, Gander Group and Davidsville Group metasediments..... 20

Figure 16: Bouguer anomaly map for the northeastern Gander Zone area; + denotes gravity station location; contour interval 1 mGal; AB, interpreted profile..... 23

Figure 17: Total-field magnetic anomaly map for the northeastern Gander Zone area; + denotes location of averaged data point; contour interval 50 nT; magnetic anomalies are relative to IGRF 1965.0; AB, interpreted profile 24

Figure 18: Uranium anomaly map for the northeastern Gander Zone area; + denotes geochemical sampling location; anomalies are in ppm; variable contour interval chosen on the basis of distribution statistics..... 25

Page

Figure 19: Nickel anomaly map for the northeastern Gander Zone area; anomalies in ppm; sampling sites same as Figure 18; variable contour interval chosen on the basis of distribution statistics..... 26

Figure 20: Residual-gravity anomaly map for the northeastern Gander Zone area; contour interval 1 mGal. AB, interpreted profile..... 27

Figure 21: Magnetic second-derivative map; contour interval 20 nT/km²..... 28

Figure 22: Compilation map for the northeastern Gander Zone geology, geophysics and geochemistry; *Dash–dot lines* indicate NW–SE breaks; *solid lines* delineate interpreted belts discussed in text..... 29

Figure 23: Gravity, magnetic and geological modelling results for profile AB (Figures 15, 16 and 17); geological symbols given in Figure 15; v, volcanics, mafic material; ∽, ultramafics; ∫ gneiss belts; +, granite.

a: Gravity model–residual gravity anomalies in mGal for profile AB denoted by x; anomalies calculated from model denoted by ○.

b: Magnetic model–magnetic anomalies for profile AB; x denotes observed magnetic anomaly, *open circle* denotes anomaly calculated from model shown in Figure 23b; *solid circle* denotes anomaly calculated from model of Figure 23b modified with top of granite at 1.5 km depth, bottom at 5.0 km and all other bodies same as Figure 23b.

c: Inferred model of subsurface geology..... 31

TABLE

Table 1: Physical properties..... 4

ABSTRACT

This report presents an interpretation of the gravity, magnetic and geochemical data for two areas of Newfoundland. One encompasses the Ackley intrusive suite of southern Newfoundland and the other covers the northeastern Gander Zone.

New gravity data were collected in both areas. These were combined with existing gravity data and analyzed in conjunction with digitized and filtered aeromagnetic data and geochemical data, to produce interpretations of the subsurface geology.

The interpretation of the Ackley intrusive suite data was accomplished by developing a 3-D gravity inversion technique utilizing vertical prisms. The density and magnetic susceptibility data were used as constraints for modelling, by examining the variation of these properties throughout the study area. By combining the potential field and physical property data, a picture of the morphology of the Ackley intrusive suite was developed.

A new technique was also developed to examine the correlation between the gravity and the lithogeochemical spatial distribution patterns. Examination of these patterns, in conjunction with the gravity and magnetic maps, suggests the presence of northwest–southeast trending lineations, which are interpreted to be of fundamental importance in controlling the emplacement of the Ackley Granite. The Dover–Hermitage Bay Fault, which bisects the study area, strongly influences the geophysical and geochemical patterns observed.

Quantitative and qualitative interpretation of the northeastern Gander Zone data suggests that there are two extensive areas underlain at depth by rocks similar to the mafic and ultramafic rocks exposed in the Gander River Ultramafic Belt (i.e., the GRUB line). These proposed regions of ultramafic and mafic rocks extend in two north–south belts throughout the study area and both have tongues continuing seaward beneath the Deadmans Bay Granite. The more westerly of the two belts, the Ocean Pond belt, probably consists of a series of granitic plutons underlain by mafic and ultramafic rocks. There is evidence from the geophysical modelling that the more easterly belt, the Indian Bay Big Pond Thrust belt, is a thrust sheet whose extent may be accurately determined, geophysically. The presence in the thrust belt of mafic and ultramafic rocks similar to typical Dunnage Zone rocks demonstrates that the GRUB line is not the most eastward exient of the Dunnage Zone in Newfoundland. The associated geochemical anomalies in Co, Ni, Pb, and Zn suggest that these may be areas for mineral exploration, since the geophysical modelling and geological mapping are consistent with the presence of the source of these geochemical patterns near the surface.

The two studies illustrate the power of interpreting geophysical, geochemical and geological data sets in the investigation of two very different and geologically complex regions. The results demonstrate that a combined geophysical and geochemical analysis is an excellent tool in predicting the geological and potential mineralization regime in areas of poor outcrop.

INTRODUCTION

This report is divided into two distinct parts, the first is a geophysical and geochemical investigation of the area, herein informally known as the Ackley intrusive suite (i.e., the Ackley Granite Suite as defined and described by Tuach, 1987) and the surrounding rocks, and the second, is a similar study of the northeastern Gander Zone of Newfoundland (Figure 1). The two study areas were the sites of major field work in 1985 (Miller, 1986), and were chosen to represent the types of problems where gravity and magnetic interpretations could contribute significantly to an understanding of the geology.

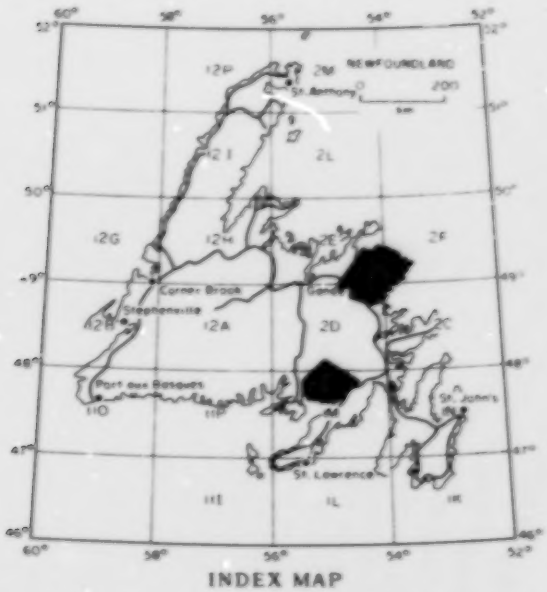

Figure 1. *Map showing Newfoundland and location of the two study sites; (1) the Ackley intrusive suite, and (2) the northeastern Gander Zone.*

The main objective of the Ackley Granite study was to determine the subsurface morphology of the granites by developing and using gravity inversion techniques. This study complements recent geological and geochemical interpretations (Tuach *et al.*, 1986, 1987; Tuach, 1987). As the study progressed, it was enlarged to develop techniques for investigating the spatial cross correlation between the three extensive geochemical, physical property and geophysical data sets for the area. These investigations made extensive use of computer data manipulation and plotting packages, some of which are commercially available and others of which, were developed during the study.

The Gander Zone study was undertaken to investigate two sets of geophysical anomalies, which were discovered by earlier work (Miller and Weir, 1982; Butler *et al.*, 1984). These earlier preliminary investigations suggested a strong correlation between the geochemical and geophysical data for the area. This study demonstrates the efficiency of a combined geochemical and geophysical interpretation in an area of poor outcrop and with only reconnaissance level geological mapping.

GEOPHYSICAL AND GEOCHEMICAL INTERPRETATION OF THE ACKLEY INTRUSIVE SUITE AND ADJOINING COUNTRY ROCKS

INTRODUCTION

The Ackley Granite area of southern Newfoundland occupies an area in excess of 2700 km² (Figure 1), astride the Dover–Hermitage Bay Fault that marks the boundary between the Gander and Avalon zones of Newfoundland. The granite hosts molybdenum and tin mineralization, and has been the subject of intensive exploration surveys. Regional lithogeochemical and geological surveys (Dickson, 1983; O'Brien *et al.*, 1984) have also been undertaken.

OBJECTIVES

The purpose of this study is to provide a geophysical data base similar in coverage to the geological and geochemical data bases, and to use all three, to obtain an understanding of the subsurface morphology and mechanisms of intrusion of the granite.

GEOLOGY AND GEOCHEMISTRY REVIEW

Initial geological mapping in the area was conducted by Bradley (1962), Jenness (1963b), Anderson (1965), Anderson and Williams (1970), and Williams (1971) who did not subdivide the granite suite into separate units. A lithogeochemical survey also did not identify separate types of granite (Strong *et al.*, 1974). However, Whalen (1976) reinterpreted the data from Strong *et al.* (1974) and suggested that there were two types of massive biotite granite and also other areas of deformed granite in the study area. A reconnaissance lake sediment geochemistry survey by Butler and Davenport (1979a, b), identified areas of anomalous molybdenum, fluorine, and uranium.

A regional lithogeochemical survey on a 4 km² grid was conducted over the Ackley intrusive suite by Dickson (1983); areas peripheral to the granite were studied by O'Brien *et al.* (1984). Tuach *et al.* (1986) and Tuach (1987) have also assessed and interpreted the geological and geochemical data. Individual granites were named by Tuach (1987) (Figure 2), and the details of the criteria used in assessing the locations of the boundaries of the various units, and the geochemical criteria for deciding upon the inclusion of specific areas, are given by him.

GEOPHYSICS REVIEW

The study area was included in the Dominion Observatory gravity survey of the island of Newfoundland

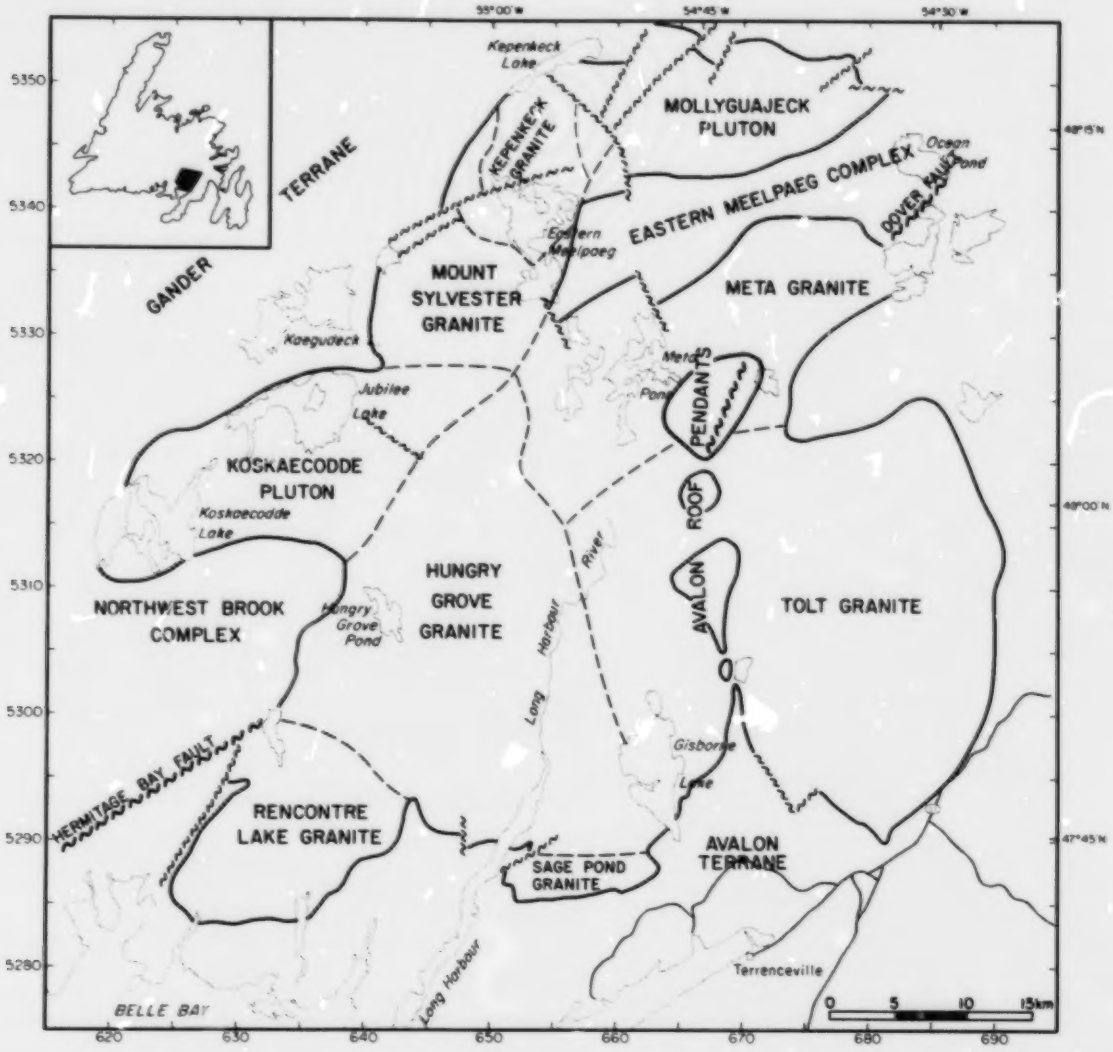

Figure 2. *Simplified geological map of Ackley intrusive suite and surrounding rocks; the nomenclature from Tuach (1987). Coordinates are UTM Zone 21, and in kilometres; map scale 1:250,000; same coordinates and scale used in Figures 3 to 10 and 12 to 14;* solid line, *external boundary of Ackley intrusive suite with country rocks;* dashed line, *internal boundaries of Ackley intrusive suite.*

(Weaver, 1967, 1968). This survey used a station spacing of 13 km with 15 stations located within the present study area. These data indicated the presence of a closed gravity low over the Ackley intrusive suite, with the most negative values located in the southeastern part of the area. However, none of Weaver's interpreted profiles traverses the present study area.

The area was also covered by the Geological Survey of Canada's aeromagnetic surveys during the 1950's and 1960's. The study area encompasses all or part of the Meta Pond, Terrenceville, Hungry Grove Pond, Mount Sylvester, Belleoram, and Gisborne Lake NTS 1:50,000 map sheets. No published interpretation of these data has been located. A search of the Newfoundland Department of Mines files, for company reports for the NTS sheets involved, indicated that ten contained geophysical information for the map areas encompassed by the present survey. These files were thoroughly examined, but none contained information on the Ackley intrusive suite.

QUALITATIVE GEOPHYSICAL INTERPRETATION

Gravity

Survey and Data Reduction: Gravity data were collected and reduced to Bouguer anomalies for 255 stations (Figure 3) following standard Earth Physics Branch (now Geological

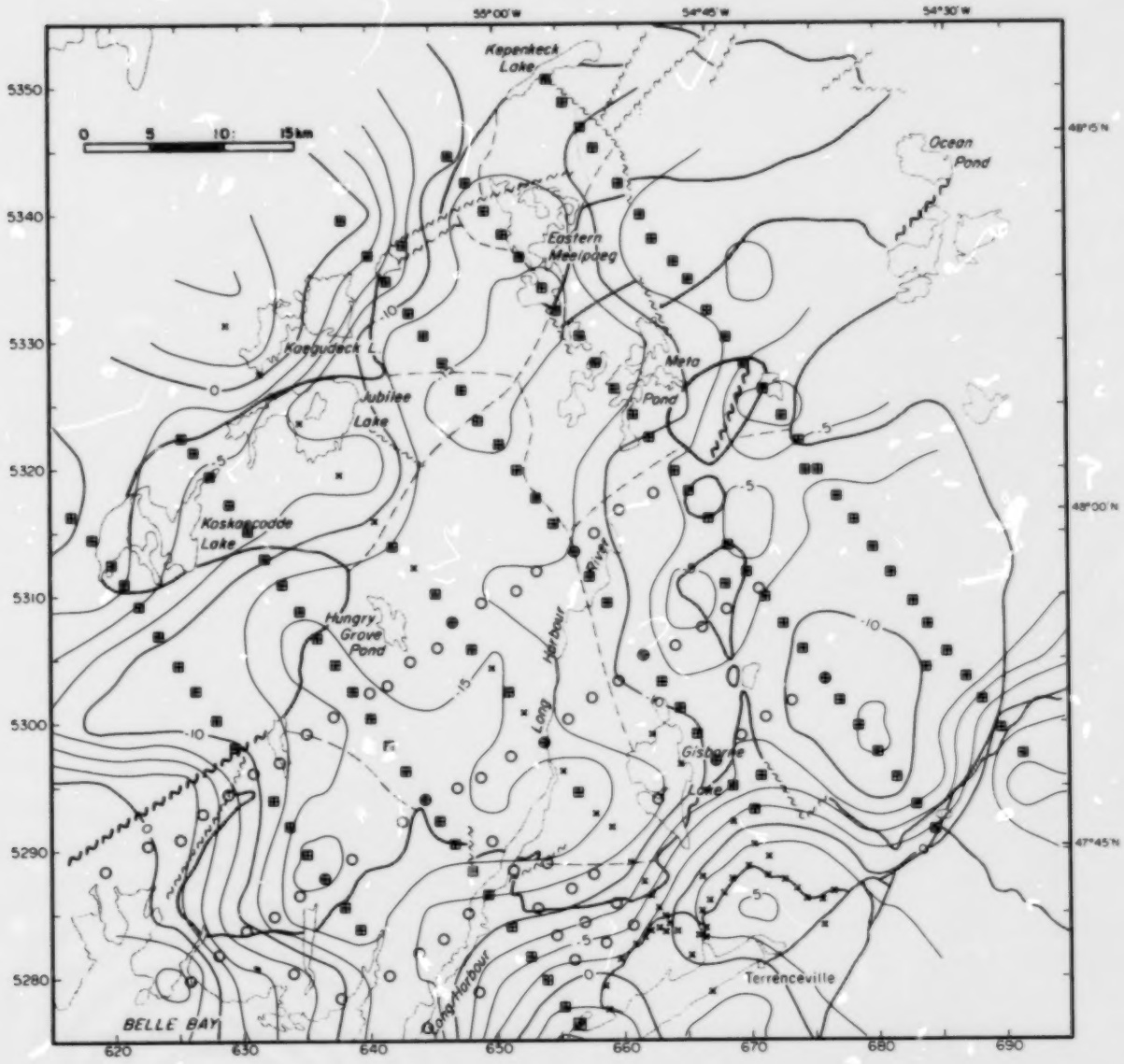

Figure 3. *Bouguer anomaly map for the Ackley study area; contour interval 2.5 mGal; X, stations from 1983 survey; ⊞ stations from 1985 survey; ○, stations from 1986 survey; geological map and coordinates same as Figure 2.*

Survey of Canada) gravity survey procedures. A preliminary survey of 52 stations in 1983 (Miller, 1983), used the Canadian National Gravity Network base at Terrenceville as the gravity and elevation base. The gravity and elevation base at Milltown was used for the 131 stations established in 1985 (Miller, 1986). During the 1985 survey, nine stations were situated at localities for which precise elevations were known, the remaining elevations were determined barometrically. An additional 72 stations tied to the Terrenceville base were occupied in 1986, to investigate areas of particular interest. Comparison of the actual elevations at bench marks with those determined barometrically at the same point, indicated that the elevation accuracy for the survey is +/− 5 m leading to an uncertainty of +/− 1.0 mGal in the Bouguer anomalies, from elevation effects. Positions were determined to +/− 25 m accuracy on 1:50,000 scale topographic maps leading to an uncertainty in the anomaly of +/− 0.04 mGal. All gravity readings were obtained with LaCoste and Romberg land G meters with a reading uncertainty of +/− 0.02 mGal. These combine to give an uncertainty of +/− 1.0 mGal in the Bouguer anomalies. The Bouguer anomaly at each station was calculated using the Canadian National Gravity Network absolute g value for the base, a crustal density of 2.67 g cm^{-3} and the 1967 International Gravity Formula (Appendix 1). The calculated Bouguer anomalies are relative to the IGSN71 (Morelli *et al.*, 1971) system and may be compared with other

Table 1. Physical Properties

Unit	No. Samples	Mean Density (g cm^{-3})	Standard Deviation (g cm^{-3})	Mean Susceptibility (10^{-3} cgs)	Standard Deviation (10^{-3} cgs)
Ackley intrusive suite					
Mount Sylvester and Kepenkeck Granites	34	2.59	0.02	0.40	0.35
Meta Granite	15	2.57	0.03	0.64	0.44
Hungry Grove Granite	115	2.56	0.03	0.22	0.26
Rencontre Lake Granite	47	2.56	0.04	0.29	0.54
Sage Pond Granite	9	2.54	0.02	0.22	0.29
Tolt Granite	86	2.57	0.10	0.37	0.29
Average	306	2.57	0.06	0.31	0.34
Associated Plutonic Rocks					
Koskaecodde Pluton	29	2.62	0.05	0.95	0.59
Eastern Meelpaeg Complex	13	2.61	0.07	0.31	0.35
Mollyguajeck Pluton	4	2.66	0.04	1.35	1.24
Northwest Brook Complex	123	2.63	0.07	0.20	1.69
Cross Hills Plutonic Suite					
(a) Gabbro/Diabase	9	2.95	0.08	4.22	4.69
(b) Granodiorite	3	2.68	0.02	0.37	0.32
(c) Alaskite/Aplite	5	2.59	0.01	0.08	0.09
(d) Peralkaline Granite	9	2.57	0.08	0.09	0.08
Average	26	2.70	0.08	1.45	2.63
Gander Zone					
Metasediments	16	2.66	0.19	0.18	0.39
Roof Pendants	4	2.63	0.05	0.63	0.59
Average	20	2.65	0.17	0.27	0.44
Avalon Zone					
Northeast Avalon	8	2.82	0.12	3.60	3.83
Southwest Avalon	7	2.68	0.16	1.40	2.71
Avalon Roof Pendants	9	2.78	0.19	0.42	0.60
Avalon Tin Lobe	5	2.76	0.17	3.32	3.56
Belle Bay	13	2.72	0.12	0.53	1.23
Average	42	2.75	0.15	1.57	2.46

anomalies determined using the same procedure and datum. Approximately −6 mGal must be added to the Weaver (1967, 1968) data to refer them to the present datum. A complete listing of all the principal facts for the gravity stations from the 1983, 1985 and 1986 surveys is available in Miller (1986). The Bouguer anomaly map for the area produced by the SURFII (Sampson, 1978) graphics package is provided in Figure 3.

Physical Properties

The physical properties were determined for 639 rock samples collected throughout the area by Dickson (1983) and Tuach (1984). The density of each rock sample was determined by weighing in air and in water. The samples were grouped according to lithological divisions (Dickson, 1983; Tuach, 1984, 1987). The mean density and magnetic susceptibilities of each unit and their respective standard deviations are presented in Table 1.

Analysis: The rocks comprising the Ackley intrusive suite as defined by Tuach (1987), i.e., the Rencontre Lake, Hungry Grove, Tolt, Mount Sylvester, Kepenkeck, Meta and Sage Pond granites, have significantly lower density than the associated plutons and the country rocks of the area (Table 1) and the lowest gravity anomalies are associated with these units. This is evident when Figure 3, the Bouguer anomaly map, is compared with Figure 4, the rock density contrast map (for which a density of 2.67 g cm^{-3} was used as reference).

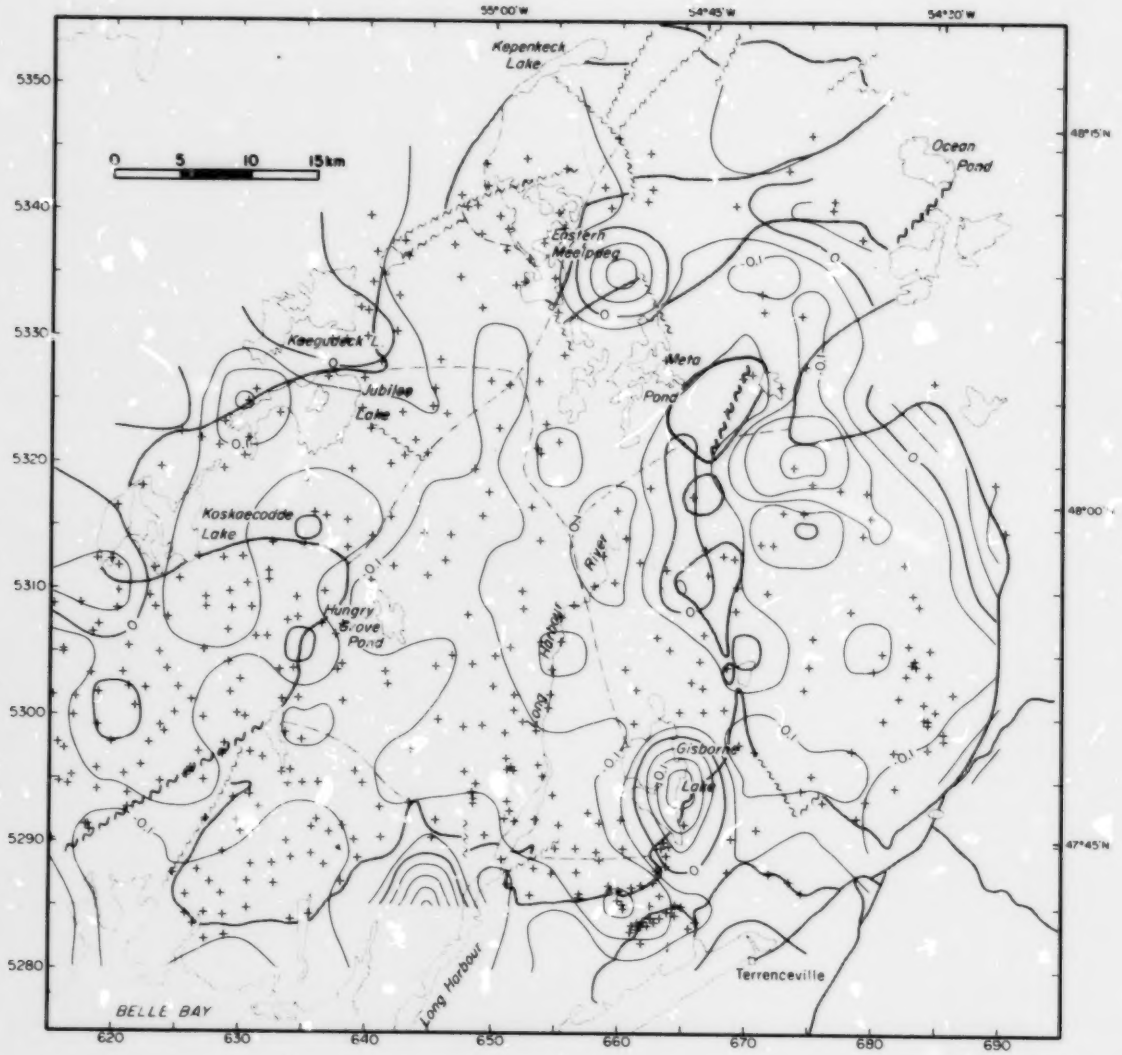

Figure 4. *Density contrast map for the Ackley study area; density contrast = rock density minus 2.67 g cm^{+3}; contour interval 0.05 g cm^{-3}.*

In the area of the Rencontre Lake Granite, the gravity anomalies reach a low of −19.7 mGal in an area where rock density contrasts lower than −0.10 g cm^{-3} are observed (Figure 4). The gravity pattern and density data are consistent with the interpretation that the subsurface limit of the southern portion of the granite suite in the Rencontre Granite is virtually in agreement with the surface geology, indicating the margin must be near vertical there.

The Hungry Grove Granite is typified by gravity anomalies in the range of −10 mGal to −17.8 mGal and density contrasts ranging from −0.05 to −0.15 g cm^{-3}. The boundaries of the granite delineated by Dickson (1983) and re-evaluated by Tuach (1987) on geochemical and lithological grounds, generally correlate well with the linear pattern of gradients in the gravity data. The areas of steep gravity gradient correlate well with density gradients, indicating that the gravity features are strongly correlated with the density values of the outcropping rocks.

The Tolt Granite is an area of direct correlation between the density and the gravity map, although neither the density nor the gravity values are as low as those attained in the Hungry Grove and Rencontre Lake granites. The outline of the unit east of the Avalon Roof Pendants is readily deduced from the gravity data, except for the northeast boundary where no gravity data are available.

The Sage Pond Granite has the lowest average density of the major granites (Table 1). Initially, only two gravity

stations were located over this pluton, and these revealed that the gravity field in the area is strongly influenced by the high density Avalon rocks immediately to the south. The boundary was accurately delineated by the gravity data collected during the 1986 survey (Figure 3). Immediately south and west of the surface boundaries of the Sage Pond Granite, the gravity anomalies are strongly negative indicating that there must be granite beneath the rhyolites of the Avalon Zone. Since the density contrast in this area is low it is difficult to calculate an accurate thickness of this granite.

The three main granites north of the Dover–Hermitage Bay Fault, the Meta Granite and the combined Mount Sylvester–Kepenkeck Granite have smaller density contrasts (Figure 4, Table 1). The Mount Sylvester Granite is typified by anomalies in the −10 to −15 mGal range and density contrasts between −0.05 and −0.10 g cm^{-3}. The Kepenkeck and Meta granites have anomalies lower than −5 mGal with associated densities mainly in the −0.05 to −0.10 g cm^{-3} range.

The adjoining associated plutons and complexes, the Koskaecodde and Mollyguajeck plutons and the Northwest Brook and Eastern Meelpaeg complexes, exhibit density characteristics different from both those of the main Ackley intrusive suite and the surrounding Avalon and Gander zone rocks (Figure 4, Table 1).

The Koskaecodde pluton is an area of less negative gravity anomalies and a mixture of positive and negative density contrasts reflecting the presence of granite and granodiorite. The Mollyguajeck pluton is typified by positive density contrasts and less negative gravity anomalies. Over the Northwest Brook and the Eastern Meelpaeg complexes, gravity anomalies are more positive than over the adjacent granites.

The gravity anomalies and density contrasts are markedly positive over most of the Avalon Zone on the southeast section of the survey area. Over the Avalon Roof Pendants, from coordinates 670E,5300N to 680E,5320N, the anomalies are tending to positive with the density contrasts also positive.

The gravity anomalies over the Gander Zone metasediments northwest of the Koskaecodde pluton are positive, but the limited density data available indicate the mean density contrast is slightly negative, although 10 of the 16 samples collected have a positive density contrast (one has a density of 2.91 g cm^{-3}). The presence of the predominantly positive anomalies indicate that the dominant density must be positive.

The gravity and density data also provide information on the location of the Dover–Hermitage Bay Fault beneath the Ackley intrusive suite. It is obvious from Figure 3 that a straight line joining the two geological segments in the northeast and southwest follows along a linear gravity feature, consistent with the presence of a fault in the northeast, from coordinates 650E,5310N to the northeast exposure of the fault.

Also evident on the gravity map are a series of northwest–southeast trending features, the most pronounced being one extending from the vicinity of 630E,5330N to 675E,5295N. Initially, these features were considered to be artifacts of the computer contouring package used; however, the additional control provided by the 1986 data along three gravity survey lines perpendicular to the initial lines and to the inferred trend confirmed that these are indeed real features. The presence of strong gradients in the gravity data associated with the trends, suggests that these may mark the location of faults along which there has been both vertical and horizontal movement. These trends will be discussed further in conjunction with the magnetic data.

The prevailing trend of the gravity pattern is exemplified by the north–south-trending gravity low in the vicinity of 650E; the density data reveal a similar pattern. The fundamental conclusion to be drawn from the analysis of the gravity and density data is that the gravity anomaly pattern is influenced primarily by the geological features mapped at the surface. Thus, inversion of the gravity data using the densities obtained from the samples will provide a reliable estimate of the subsurface topology of the granite. The quantitative analysis will be discussed further following discussion of the qualitative magnetic interpretation.

Magnetics

Techniques: The data used for the aeromagnetic interpretation consist of the GSC 1:63360 aeromagnetic maps for Meta Pond, Terrenceville, Belleoram, Mount Sylvester, Kepenkeck Lake, Hungry Grove Pond, and Gisborne Lake map areas[1]. These maps are based upon surveys flown at an elevation of 1000 ft. (305 m) with east–west flight lines separated by 0.5 mi (0.805 km). The data for the Mount Sylvester and Meta Pond maps were collected using fluxgate magnetometers and are total field data, referenced to an arbitrary datum. The remaining maps were produced from total field data collected using proton precession magnetometers yielding absolute total field values. The Meta Pond and Mount Sylvester data were adjusted to absolute total field values by comparing the data along the boundaries of these maps with that of adjoining absolute total field maps and determining a linear regression equation (Appendix 2). After applying this correction, all maps were digitized using a 0.5 mi (0.805 km) digitizing interval in both the east–west and north–south directions and the datum correction added. The processing sequence is discussed in detail in Appendix 2 and the magnetic total field anomaly map is presented in Figure 5.

[1] GSC 1:63360 Aeromagnetic Map Numbers 203, 4512, 4511, 202, 192, 4497 and 4498 respectively.

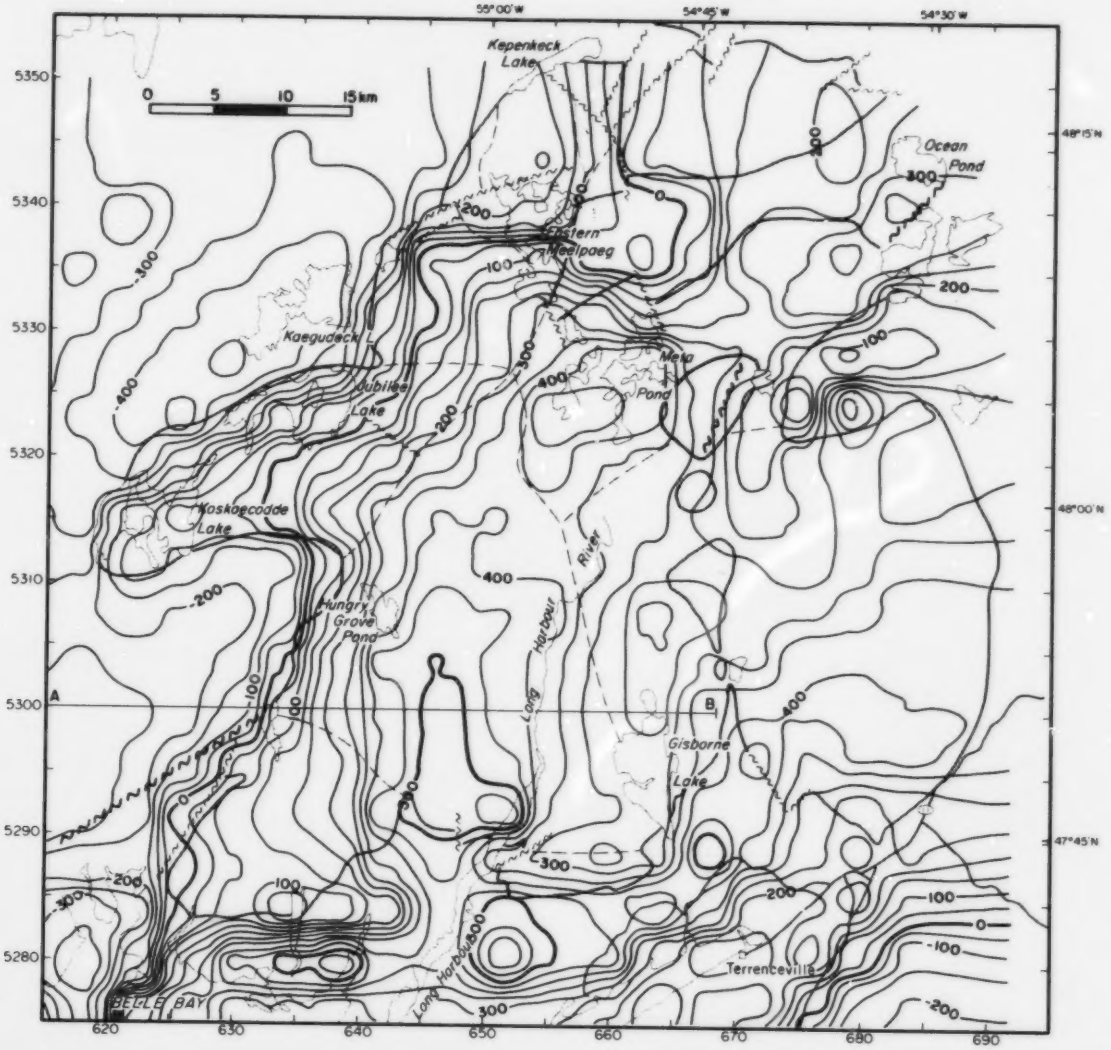

Figure 5. *Total-field magnetic anomaly map for the Ackley study area based on 4 km filtered data (technique discussed in Appendix 2); contour interval 50 nT; AB, interpreted profile.*

The magnetic susceptibility of each rock sample was measured using a portable susceptibility meter. The mean susceptibility and the standard deviation for each of the units were calculated (Table 1) and a susceptibility map was plotted using the SURFII package (Figure 6).

The relationship between the boundaries of the causative bodies and the magnetic anomalies was investigated by producing a second-derivative map, (Figure 7). This map was prepared from the digitized data by filtering, to produce 4-km averaged magnetic data using an approach described in Appendix 2. The filtered data have a wavelength similar to the gravity data. The second-derivative method, enhancing the location of inflection points in the magnetic map, enables one to determine magnetic boundaries more readily and to discern subtle trends in the data, as it may be shown that this procedure is also similar to a regional–residual separation technique (Henderson and Zeitz, 1967, and Appendix 2).

Analysis: Comparison of the two maps (Figures 5 and 6) and consideration of the data of Table 1 suggest that the major units of the Ackley intrusive suite, the Rencontre Lake, Hungry Grove, Sage Pond, and Tolt granites have lower magnetic susceptibility relative to those of the other units in the area, especially the Avalon Zone rocks. This is particularly true of the Hungry Grove Granite, south of the Dover–Hermitage Bay Fault and of the Rencontre Lake and Tolt granites and implies that the north–south-trending positive magnetic anomaly, with a maximum amplitude in excess of 600 nT in the area of the Hungry Grove Granite, must be caused not by the granite itself but by magnetic rocks beneath the granite. The presence of Avalon Zone mafic rocks

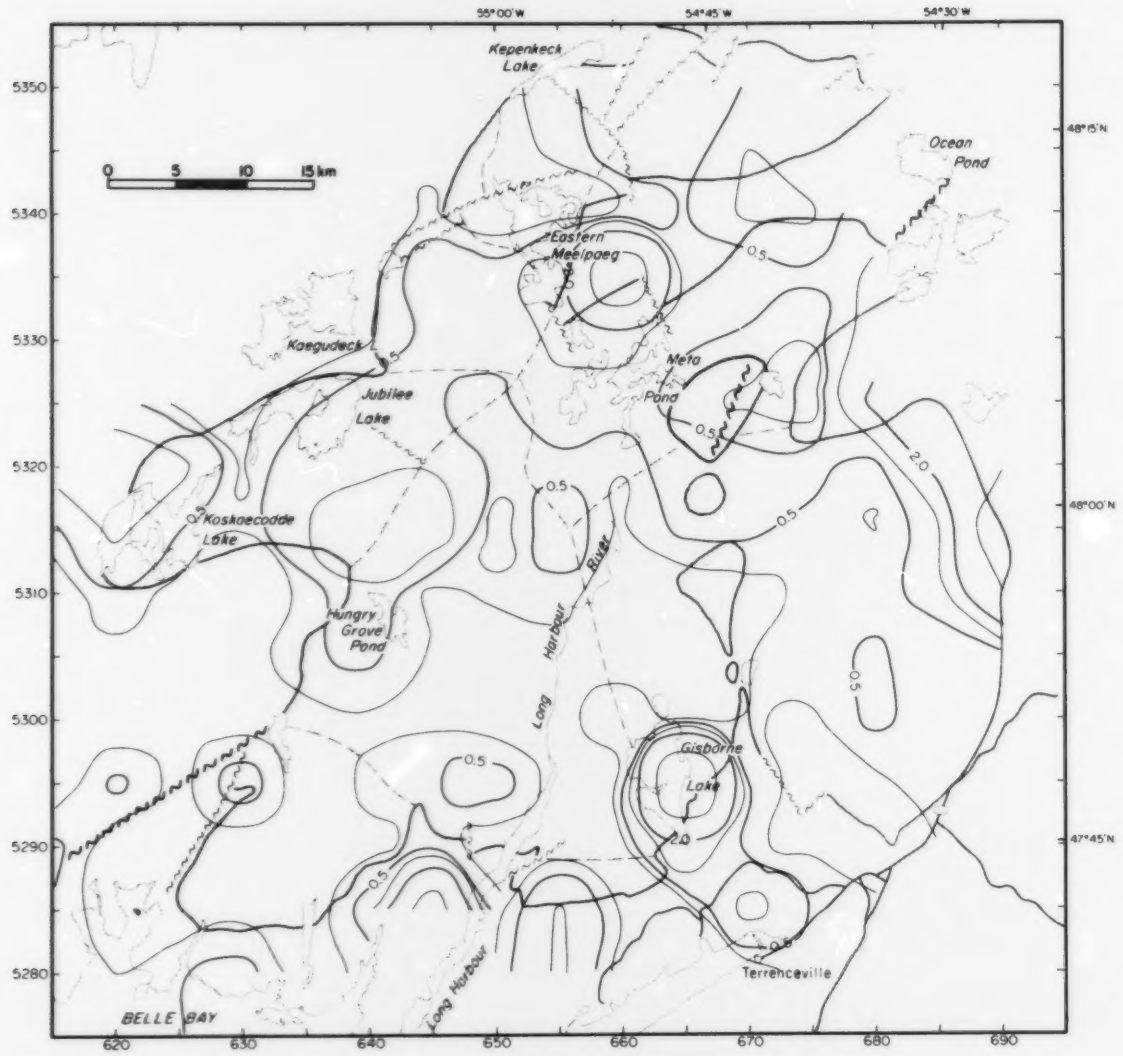

Figure 6. *Magnetic susceptibility map for the Ackley study area; contours drawn at 0.25, 0.5, 1.0, 2.0, 4.0 cgs susceptibility units.*

beneath the Hungry Grove Granite is deduced from the similarity in amplitude between this north-trending anomaly and the anomalies over the Avalon mafic rocks to the south. The nature of the magnetic pattern around the Hungry Grove Granite is suggestive of faulting at depth on the west, south and east sides of the body.

The trace of the Dover–Hermitage Bay Fault is discernible on the magnetic map (Figure 5) where contours in the northern half of the Hungry Grove Granite have a more northeasterly trend that contrasts with the overall northerly trend of the associated positive anomaly. On the magnetic susceptibility map (Figure 6) the magnetic susceptibility of the surface samples is also higher north of the fault. The more complicated susceptibility pattern north of the fault, correlates with magnetic anomalies and indicates that the sources of the anomalies are the rocks exposed at the surface.

The Gander Zone rocks are the least magnetic of any in the survey area and are associated with the large magnetic low in the northwest corner of the survey area. This magnetic low is part of the regional magnetic low typical of the Gander Zone (Haworth and Jacobi, 1983). Magnetic anomalies over the Avalon Zone in the southeastern section of the study area are strongly positive over mafic volcanics and negative in areas of acid volcanics. This association of strong magnetic anomalies with areas of Precambrian volcanics is typical of the Avalon Zone (Miller, 1983, 1985, 1986; Haworth and Lefort, 1979).

The dominant feature of the magnetic second-derivative map (Figure 7) is the linear northeast-trending valley along the interpolated location of the Dover–Hermitage Bay Fault. This supports the interpretation that the fault exists both at depth beneath the Ackley intrusive suite and at the surface,

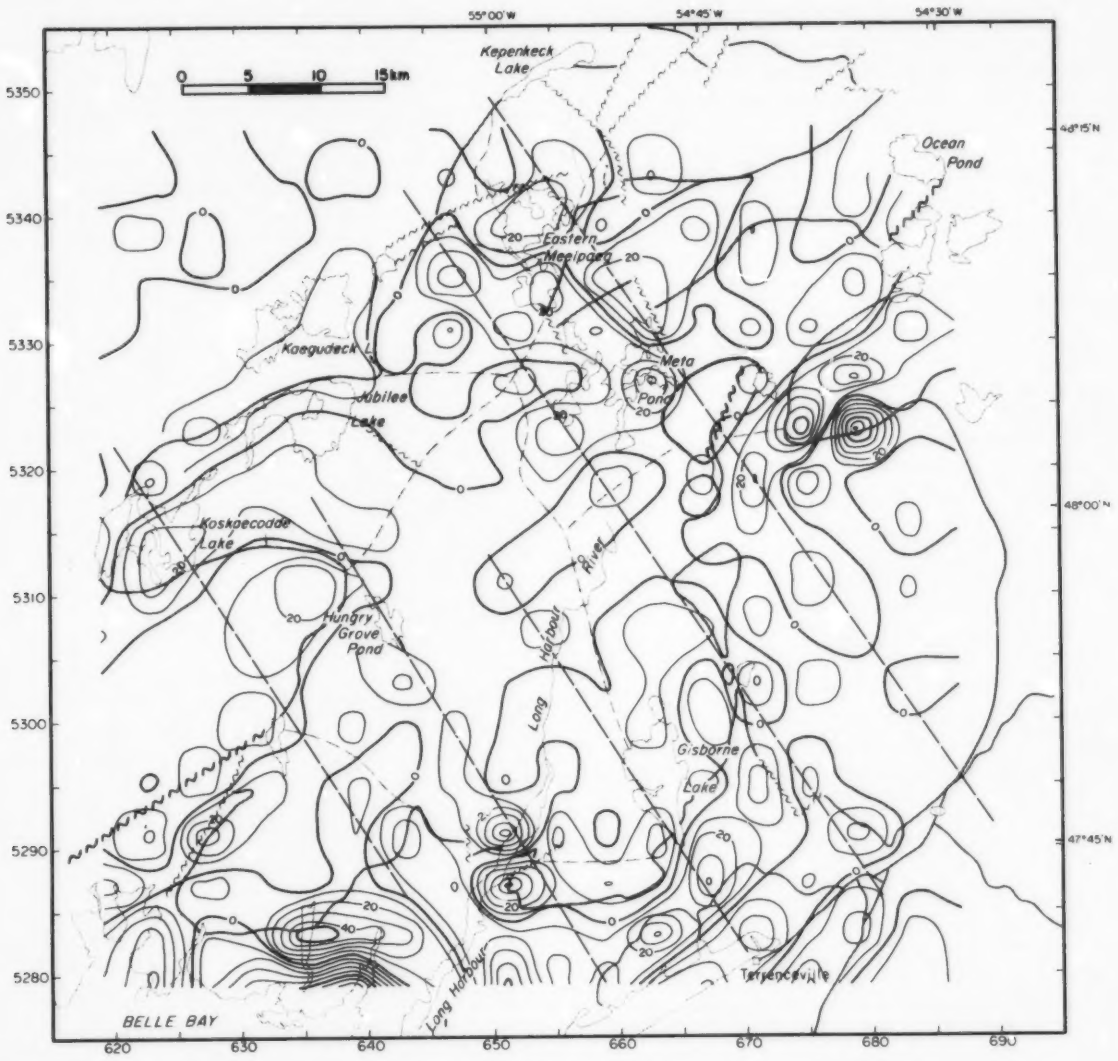

Figure 7. *Second-derivative magnetic map for the Ackley study area; contour interval 10 nT/km².*

and separates two areas of differing magnetic properties as inferred from both the magnetic and the susceptibility map.

The magnetic second-derivative map (Figure 7) also exhibits northwest–southeast lineations in the same locations as initially suggested by the gravity data (Figures 3 and 4). This provides additional evidence for the physical significance of such features. The presence of these features in the magnetic data, in the area of the Hungry Grove Granite where the magnetic signatures are interpreted to be caused by material beneath the granite, suggests that they were formed prior to, or contemporaneous with, the emplacement of the granite, and are related to faulting in the Avalon basement beneath the southern portion of the Ackley intrusive suite.

The magnetic maps (Figures 5, 6 and 7) and Table 1 demonstrate the contrast between the northern granites, (i.e., the Mount Sylvester, Kepenkeck and Meta granites), and the southern granites, (i.e., the Rencontre Lake, Hungry Grove, Tolt and Sage Pond granites). In general, the magnetic susceptibilities and densities of these northern granites are higher and more variable.

QUANTITATIVE GEOPHYSICAL INTERPRETATION

2½-D Inversion

The objective of the quantitative gravity interpretation is to determine the morphology of the granite using the gravity and density data. Two approaches were used, a 2½-D inversion method developed by Peavy (1985) and a 3-D inversion method developed as part of this study (Appendix 3).

Technique: The inversion methods were used to determine the thickness of material of the specified density required to explain the observed anomaly. Where the particular rock type outcrops, the thickness and depth are synonymous; the depth is the depth immediately below the surface.

The 2½-D inversion method uses a constant density contrast of -0.10 g cm^{-3} and can only operate on anomalies that are all negative. It determines the thickness of the granite, in kilometres, at each observed data point from the 2-D slab expression, $\Delta g = 41.9\ \Delta\varrho\ t$, and constructs a body having x coordinates given by the x coordinate of the observation point and z coordinate determined by the expression $g(x) = 41.9\ \Delta\varrho\ z(x)$. The program then uses the Rasmusen and Pedersen (1979) algorithm, to compute the gravity effect of a body having this cross-section and a 10 km-strike length, with 5 km on each side of the profile since the survey lines are 10 km apart. The computed and observed gravity results are compared and an adjustment to the thickness is determined from,

$$\Delta Z(x) = \frac{\Delta g_{OBS} - \Delta g_{calc}}{41.9\ \Delta\varrho}$$

This adjustment in thickness is applied not only to the thickness at the horizontal location of the data point but also at adjacent locations using a cosine bell filter (Peavy, 1985). This approach smooths the depth and reduces the tendency of such an inversion scheme to dig deep holes at the edges of the body. The choice of an appropriate filter width is a subjective judgement based on previous experience, and in the present study a width of 10 km was chosen.

Analysis: The granite thickness map (Figure 8), determined from the data along the six northwest–southeast profiles, demonstrates that the thickest portions of the Ackley intrusive suite are associated with the Mount Sylvester Granite in the northwestern section of the survey area, and the Rencontre Lake and Sage Pond granites in the south. No southwest–northeast profiles were inverted as the two profiles that traverse the Rencontre Lake Granite, skirt too close to the boundaries to yield valid results. The deepest portion of the main Ackley intrusive suite, at 10 km depth, occurs just inside the Rencontre Lake Granite. The 2½-D depth data, together with the contoured gravity data, indicate that there must be a significant thickness of granite beneath those portions of the Avalon Zone, to the west of the Sage Pond Granite and south of the Rencontre Lake Granite. This suggests that a lobe of the granite, with which mineralization is associated, is intruded beneath part of the Avalon Zone and that the granite must have a greater extent than that evident by surface outcrop. A similar conclusion may be drawn for the Hungry Grove Granite and Northwest Brook Complex contact, where it appears from the inversion results that there may be granite beneath the Northwest Brook Complex.

The Avalon Roof Pendants must be areas of extremely thin granite, which exist beneath the exposed pendant rocks and there is a deep lobe in the southern portion of the Tolt Granite.

There is relatively good correlation between the major gradients in the depth contours and the boundaries of the Ackley intrusive suite with the adjacent rocks, indicating that the inversion process is a viable method for delineating the margins of the granite. From the data presented, it is seen that the minimum thickness in the main section of the granite is approximately 4 km, with the central portions having a thickness of about 5 km, and the deep lobes near the boundaries reaching depths greater than 7 km.

The propensity of the inversion scheme for creating deep lobes near the edges of bodies, casts some doubts on the absolute depth of the lobes in the Hungry Grove Granite, near its boundaries with the Northwest Brook Complex and the Koskaecodde pluton, and on the depth of the Rencontre and Sage Pond granites adjacent to the Avalon Zone rocks on the southeastern edge of the study area. In an effort to resolve these questions, a 3-D inversion method was developed as part of the interpretation of the Ackley intrusive suite.

3-D Inversion

Technique: This inversion method, developed as a part of the present study, is described in Appendix 3. The procedure uses the SURFII package to interpolate both the density and gravity data onto a regular, rectangular grid whose boundaries are given by the gravity lines. Both gravity and density data sets are rotated to a new coordinate system (Appendix 3) and then the gridding package of SURFII used. This results in two data sets G(x,y), gravity, and D(x,y), density, each having a data point at locations N Δx, M Δy where Δx, Δy = 5 km. These two data values at the same location may then be used to calculate the initial estimate of the thickness T(x,y) of a 5 km x 5 km x T(x,y) vertical prism centred on x,y, which causes the observed anomaly G(x,y).

The initial estimate of thickness of each prism T(x,y) is calculated from the following expression derived in Appendix 3.

$$0.5\ G(x,y) = 103.4\ D(x,y)\ [1 - \exp(-T(x,y)/2.5)]$$

The gravity effect at each location N Δx, M Δy is calculated as the sum of the effect of the prism immediately underlying the point N Δx, M Δy and from the effects at the location N Δx, M Δy for the 48 prisms in the immediate vicinity, i.e., centred at (N+l) Δx, (M+k) Δy where l,k = 0,1,2,3. Testing for typical dimension prisms revealed that the effects of prisms at greater distances contributed a total effect less than the uncertainty in observed g, i.e., less than +/− 1.0 mGal (Appendix 3).

After the gravity effect at each location is calculated, it is compared with the observed Bouguer anomaly and the mean difference and the standard deviation of the differences are calculated. If the standard deviation of the differences

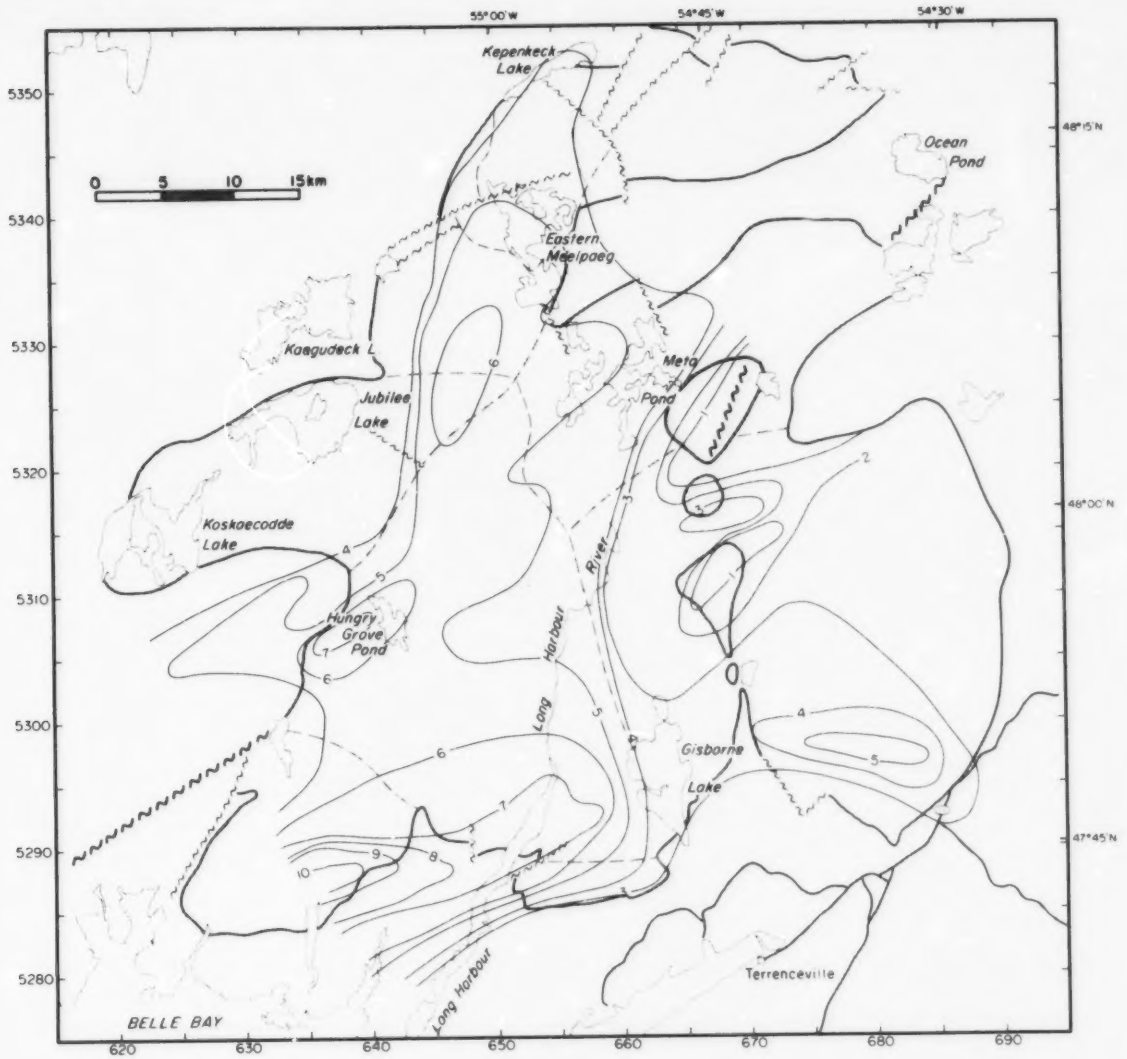

Figure 8. *Granite thickness map from 2½-D inversion for the Ackley study area; contour interval 1.0 km.*

is less than +/− 1.0 mGal, the process terminates. If not, each thickness is incremented by an amount

$$T(x,y) = \frac{2 * [\Delta g_{OBS}(x,y) - \Delta g_{calc}(x,y)]}{41.9\ D(x,y)}$$

which is twice the 2-D slab increment. This larger value was used since the 2-D slab iteration assumes the mass extends infinitely in the horizontal direction, which is not the case here, and consequently a smaller thickness adjustment than for vertical prism is obtained. Using the 2-D slab iteration would result in slow convergence, and using the derivative of the expression used for calculating the initial thickness results in a T which is very unstable. The iteration to the thickness at each location is added to the thickness at the location from the previous iteration to give $T_i+1\ (x,y) = T_i\ (x,y) + \Delta\ T_i\ (x,y)$ where i, is iteration number.

This new thickness estimate is then run through a smoothing filter, the effect of which is to distribute the changes in depth partly to surrounding points to reflect the dependence of the gravity anomaly at (x,y) on mass distributions not only immediately beneath (x,y) but at surrounding locations. The filter used is a simple weighting filter having weights 0.7, 0.04375 and 0.03125, at distances 0, 1 and $\sqrt{2}$ respectively. The smoothed thicknesses $T_*(x,y)$ are then used to compute the gravity effect in the same manner as the initial calculation. The process continues in such a loop until the standard deviation of the difference between the observed and calculated anomalies is less than 1.0 mGal or until a maximum specified number of iterations is completed. The statistics for each iteration are examined in the second case and the iteration that produced the minimum variance is chosen. In practice, this was achieved in fewer than ten iterations when the data were run using the observed density and gravity data. The resulting thickness map is presented in Figure 9.

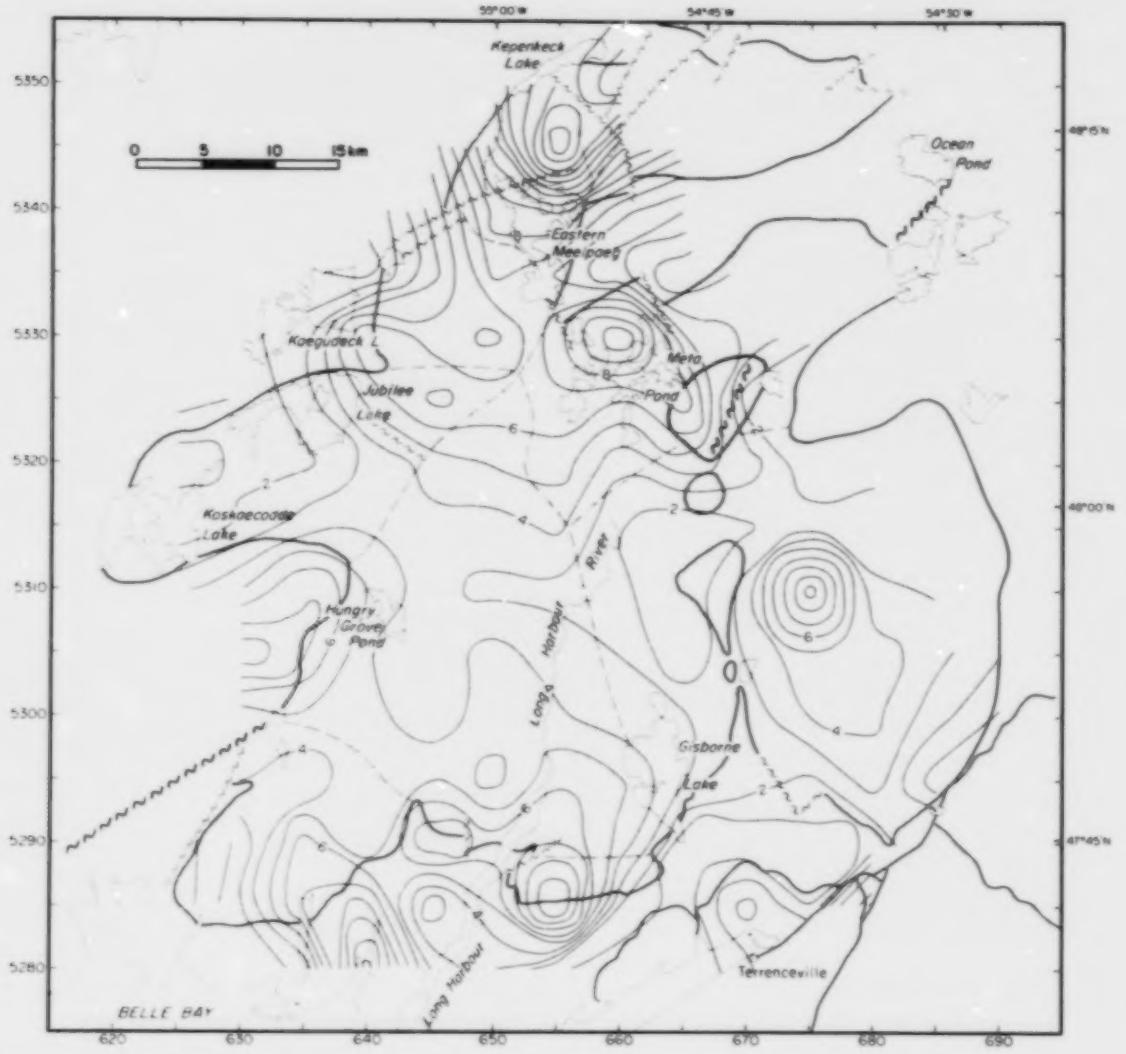

Figure 9. *Granite thickness for the Ackley study area from 3-D inversion method with variable density; contour interval 1.0 km.*

The advantage of the 3-D inversion over the 2½-D method is that it can handle both positive and negative density contrasts and positive and negative anomalies. The main disadvantage of using the observed interpolated density contrast is that in areas where the magnitude of the density contrast is small, the calculated thickness will be large. This is partly ameliorated by the smoothing filter, but it still means that the depth is dependent on the density contrast at that location. The fundamental assumption made in this method, is that the density observed at the surface at a given location, is typical of the density in a 5 km x 5 km x T km prism centred at that location, and extending from the surface to the bottom of the body. This is an unlikely event for this granite suite (Tuach *et al.*, 1986) with its degree of chemical inhomogeneity.

Examination of Figure 9 shows that the extremes of depth in the main portion of the Ackley intrusive suite are not as great as depicted in Figure 8. The same major lobes still appear, giving credence to their existence as real features and not just artifacts of the 2½-D inversion scheme. The major difference on this map is that thickness estimates for the adjoining plutons and the positive density areas are now given by examining the contours in those areas. This map is most noticeably different from the previous one in the Long Harbour area between the Rencontre Lake and Sage Pond granites where there is now less evidence of the granite undercutting the Avalon Zone rocks. This results from the presence of positive density rocks in the Avalon Zone. However, there is still a deep lobe associated with the southern boundary of the main Ackley intrusive suite, another

associated with the Kepenkeck Granite, and yet another associated with the Tolt Granite. The deepest portion of this model is in the Meta Granite where it must be noted that the density contrast is small. This, coupled with a significantly negative gravity anomaly, leads to a large depth estimate of 10 km. In the vicinity of 630E,5305N, a similar deep lobe occurs, which may also be explained by small negative density effects (c.f. Figure 4). A major feature not seen as prominently on the 2½-D inversion map is the east–west ridge in the Hungry Grove Granite at approximately 5310N. This is the area of a similar east–west extreme low in density (Figure 4), so one expects a shallower depth there.

The density data for the area (Table 1) suggest a considerable degree of homogeneity in individual units. Because the assumption of constant density over a vertical section is a restrictive and not necessarily valid assumption, it was decided to run the 3-D inversion method using a constant density contrast of -0.10 g cm^{-3} where the gridded density contrast was negative, and a density contrast of $+0.10$ g cm^{-3} where the gridded density contrast was positive. This approach resulted in the thickness map of Figure 10.

This map (Figure 10) does not have the extreme lobes of the previous two maps (Figures 8 and 9). However, it does indicate that the Ackley intrusive suite is the area of greatest granite thickness and the deep lobes associated with its boundaries are still present, although smaller both in amplitude and area. Perhaps most significantly the deepest lobe is now associated with the most negative gravity anomaly in the Rencontre Lake Granite. This map also indicates significant undercutting of the Avalon in the Rencontre Lake Granite and Sage Pond Granite. It suggests a flat bottom in the main Hungry Grove Granite and that the Tolt Granite has a deep, albeit thinner lobe than the other two inversion results suggest (Figures 8 and 9). The depth in the Kepenkeck Granite is still greater since the density contrast used is an average value.

This model is preferred over the others; it is most consistent with the average density of the main Ackley intrusive suite, which Table 1 shows, and which Figure 4 demonstrates is fairly homogeneous in its density, both, statistically and spatially.

Magnetic Modelling

So far, the interpretation has been based upon inversion of the gravity data only. In the earlier discussion of the magnetic data it was concluded that Avalon type mafic volcanics must underlie the Hungry Grove Granite.

The profile AB (Figures 5 and 11) was chosen for modelling since it is perpendicular to the main anomaly associated with the area of the Hungry Grove Granite. Using a susceptibility contrast of 8×10^{-3} cgs units, which is consistent with the upper range of the Avalon data (Table 1) and the mapped susceptibility (Figure 6), good agreement was obtained between the observed and calculated magnetic data if a block of magnetic material interpreted as Avalon mafic rocks, is placed with its top at a depth compatible with the 3-D inverted gravity data for the bottom Hungry Grove Granite. The top of the block dips eastward and is fault bounded at the location of the boundary between the Hungry Grove Granite and the Tolt Granite in the vicinity of the Avalon Roof Pendants. East of this area, there must be Avalon material close to surface, i.e., the Avalon Roof Pendants. The model is not really valid east of the roof pendant area as the anomaly pattern is parallel to the profile.

An alternate interpretation is that the magnetic field could be caused by enhanced susceptibility in the granite itself and not by any underlying rocks. This possibility was modelled by assigning a susceptibility of 0.5×10^{-3} cgs to the granite, approximately twice that of the mean in Table 1. The calculated magnetic field was of insignificant amplitude and of completely different geometry than the observed field.

These models support the qualitative interpretation that the magnetic anomaly in the Hungry Grove Granite area is due to the presence of downfaulted Avalon Zone mafic material beneath the granite. The agreement between the depth of the granite calculated from the gravity inversion process, and the top of the underlying Avalon Zone material determined from the magnetic data, further corroborates the interpretation as the magnetic modelling was conducted independent of the gravity inversion.

The presence of the interpreted volcanics beneath the granite would normally cause a positive gravity anomaly. But geological evidence (O'Brien *et al.*, 1984) suggests that there is a considerable rhyolite constituent to the volcanics and the density of Avalon rhyolites is close to 2.67 g cm^{-3}, leading to negligible contribution to the gravity.

COMBINED GEOPHYSICAL AND GEOCHEMICAL INTERPRETATION

Technique

The existence of the large geochemical sample database for the area provides an opportunity to examine the degree of cross correlation between the geophysical and geochemical data on a quantitative basis. The cross correlation between the physical properties and the geochemical analyses can be rapidly computed using the Pearson product moment correlation coefficient (Hays and Winkler, 1970), since both used the same samples. In the situation under consideration here, it is desirable to be able to examine the spatial distribution of the correlation between the two variables, i.e., to be able to locate on a geographical map where the correlation between the two variables is either strong or weak. It may be argued that this is possible by overlaying the two maps of the appropriate variables, but such a method gives no quantitative indication of the strength of the correlation. Accordingly a modification of the normal process of determining the correlation coefficient was developed (Appendix 4), which enables a correlation factor, r_{ij}, to be determined for each sample location wherein data for each of the two variables being correlated are available. Then a map of the r_{ij}'s can be produced where

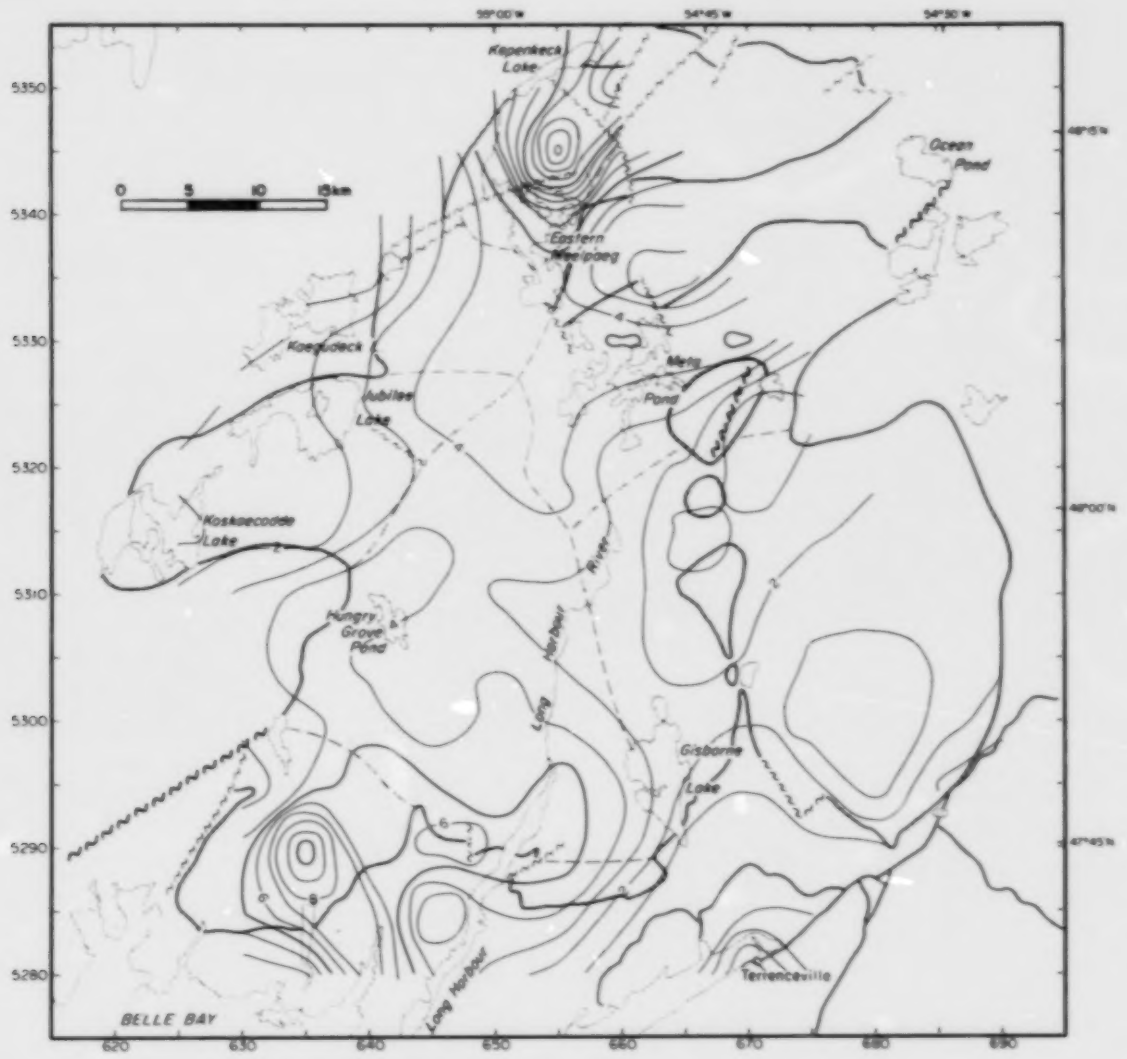

Figure 10. *Granite thickness for the Ackley study area from 3-D inversion method with constant density; contour interval 1.0 km.*

$$r_{ij} = \frac{(x_{ij}-\bar{x})}{Sx}\,\frac{(y_{ij}-\bar{y})}{Sy}$$

(standard Z score for x)* (standard Z score for y)

Areas where r_{ij} has a large absolute value are areas where both variables differ significantly from their mean values and are areas warranting close scrutiny for the source of the anomalous values.

The major problem with using such an approach with either the magnetic or gravity data, compared with either of the physical properties or the geochemical data is that the geophysical and other data were not necessarily collected at the same locations. This problem is overcome by using the GRID function of the SURFII package to interpolate both data sets onto the same grid (Appendix 4). Then the grid data can readily be compared, point by point, and both the Pearson correlation coefficient, r_{xy}, and the modified correlation factor, r_{ij}, can be determined for the data sets as a whole and for each point respectively.

This procedure was used to examine the correlation between the density and gravity data, the gravity and silica concentrations, the density and silica concentrations, and the gravity and each of the rubidium, fluorine and uranium concentrations.

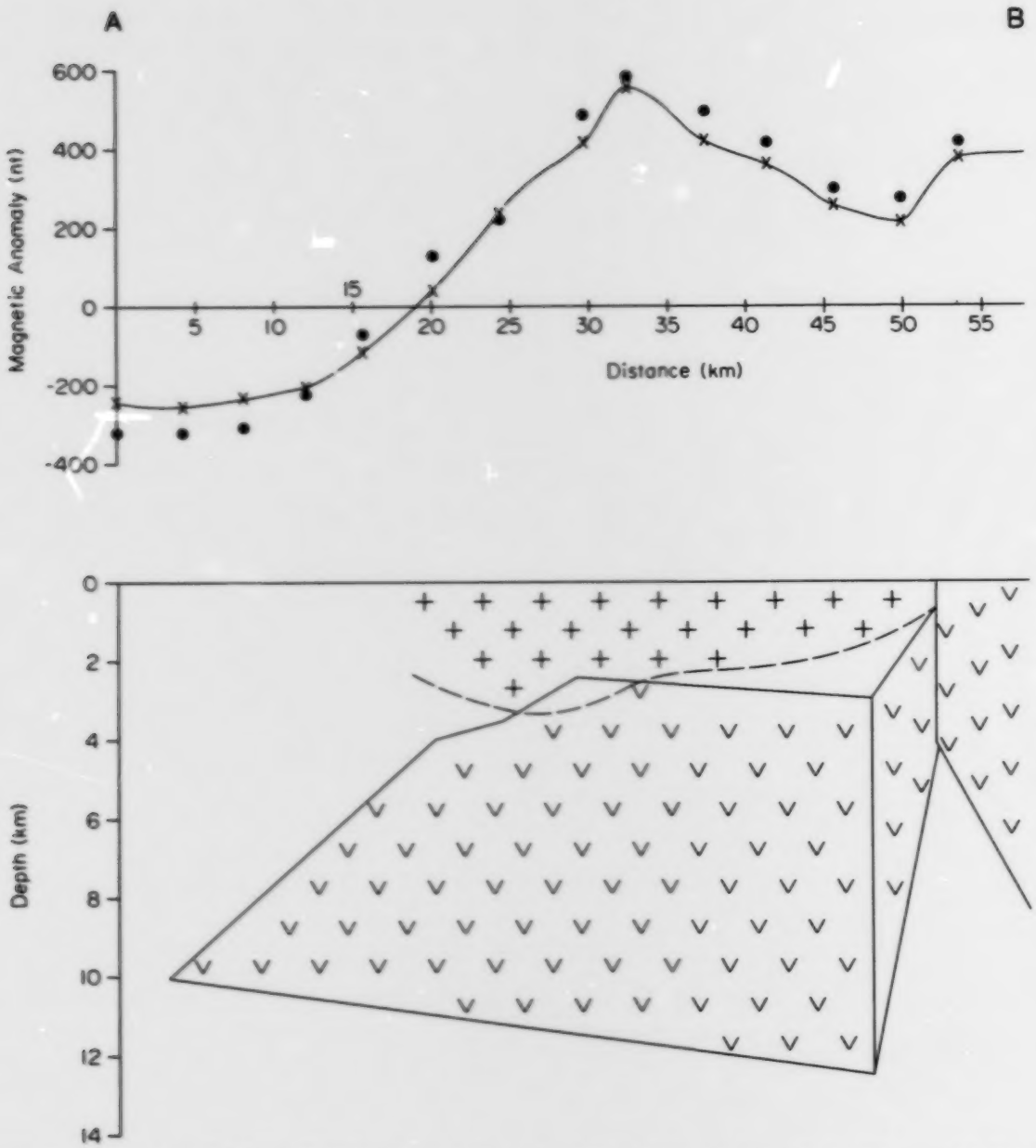

Figure 11. *Magnetic model for profile AB on Figure 5; X, observed filtered data;* •*, data calculated from model.* VV *Avalon Roof Pendants, + granitic rocks; geological boundaries shown;* solid line, *magnetic body;* dashed line, *bottom of granite from Figure 10.*

Analysis

Gravity–Density Correlation: As discussed earlier, there is a high degree of correlation between the two data sets. The Pearson correlation coefficient, r_{xy}, for the two (based upon a grid having 5-km spacing, i.e., the same grid used for the 3-D inversion) is 0.152, which indicates a significant degree of correlation at better than 95 percent probability. The spatial distribution of r_{ij} (Figure 12) indicates that for most of the area the correlation is low positive and neither variable varies significantly from the mean value. In parts of the grid, there are extremes in the correlation score that correlate primarily with low gravity values. One particular spot location at 640N,5290E exhibits an r_{ij} factor of −5.14 indicating an extreme positive density in the vicinity of a gravity low. Examination of the data suggests the interpolated density here

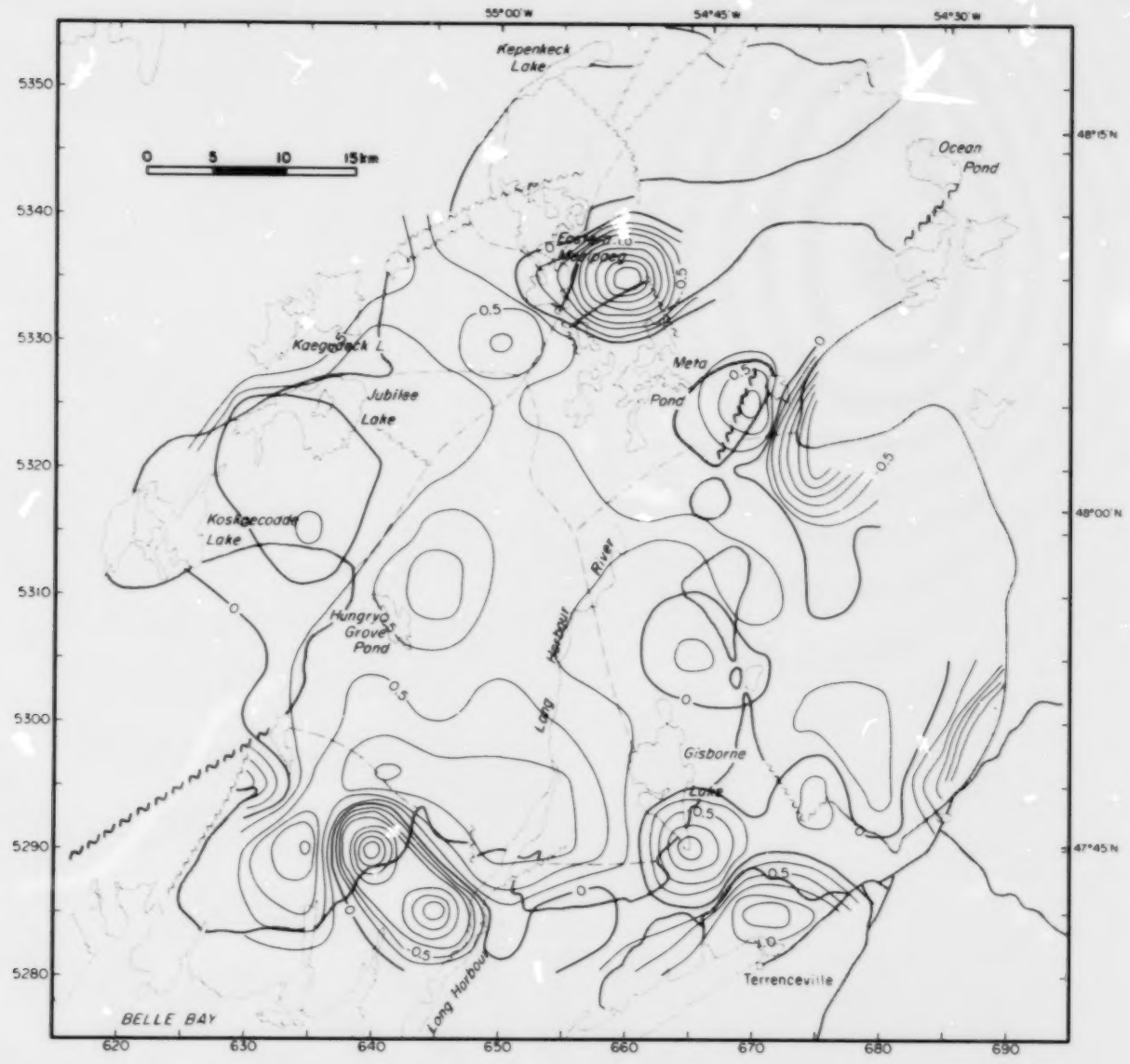

Figure 12. *Gravity–density correlation map for the Ackley study area; contour interval 0.25.*

is high because there is a single extremely high density sample in that area. Other significantly negative correlations occur outside the main granite in the Eastern Meelpaeg Complex and in the Avalon Zone rocks south of Gisborne Lake. The general nature of the geographical distribution of the correlation function, substantiates the earlier interpretation that the gravity field is controlled primarily by the density of the rocks exposed at surface.

Silica–Density and Silica–Gravity Correlations: Given the high degree of correlation between the density and gravity data, it is not surprising that the Pearson coefficients for the silica–gravity and silica–density correlations are almost identical, being −0.208 and −0.223 respectively. Both of these are significant correlations at greater than the 99 percent confidence levels. These results indicate that the density decreases as the silica content increases, and that the gravity becomes more negative with increasing silica content, and therefore the more negative density contrast. In both of these cases, where r_{ij} is negative, the areas of most significance are areas where r_{ij} is positive, i.e., going against the trend and in areas where r_{ij} is of high negative amplitude. The major features of the silica–gravity correlation map (Figure 13) are the positive correlation north of the Dover–Hermitage Bay Fault, the north trend at 650E, and the strong negative correlation trend around the southern boundary of the Hungry

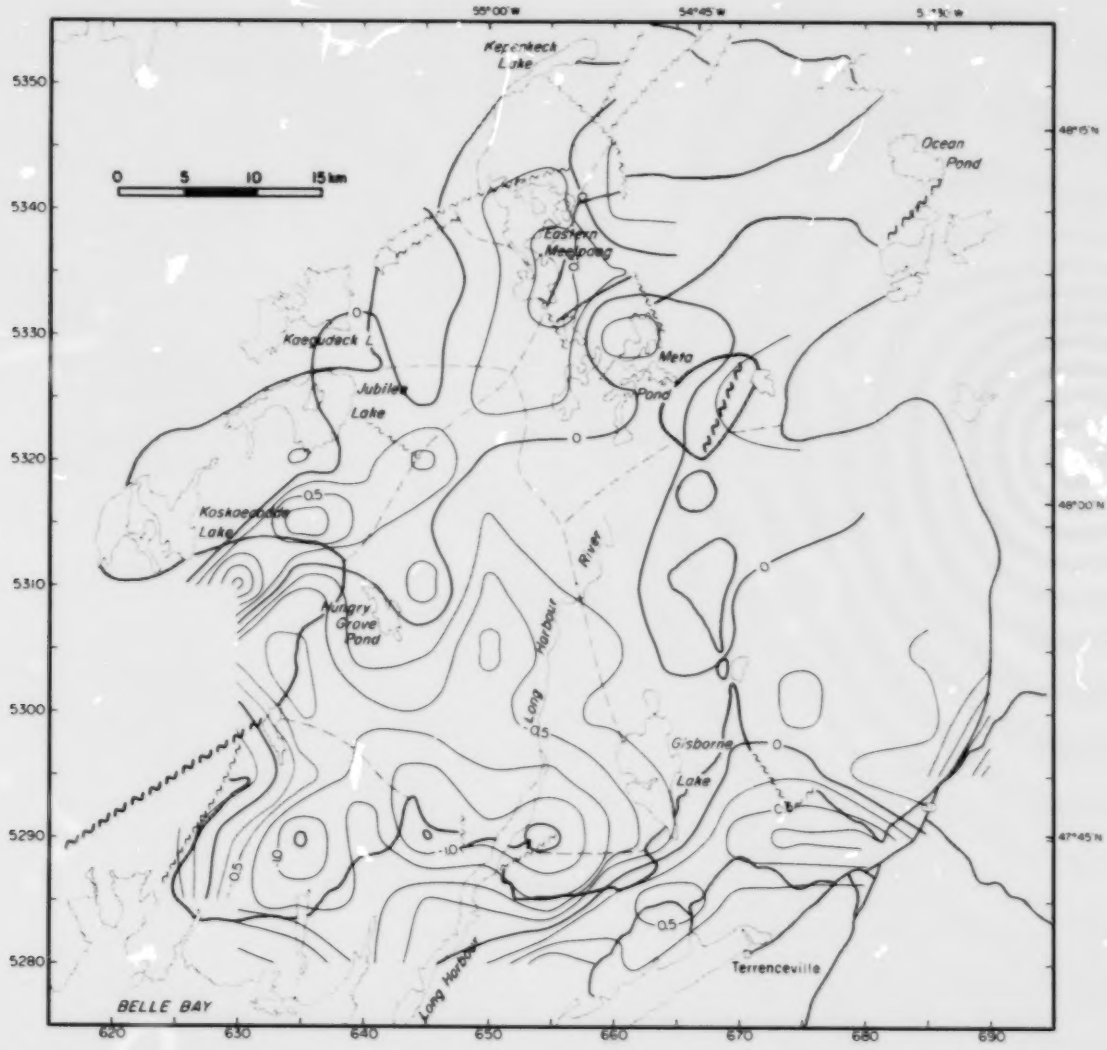

Figure 13. *Silica–gravity correlation map for the Ackley study area; contour interval 0.25.*

Grove Granite and in the middle of the Rencontre Lake Granite. These areas of negative correlation suggest that low density, high silica granite is found there. The change in character of the correlation function across the Dover–Hermitage Bay Fault suggests that the general chemical nature of the rocks changes north of the fault. The north–trending pattern in the silica–gravity correlation pattern parallels the same trend in the gravity data. The correlations demonstrate that the silica distribution is one of the primary factors influencing the rock density.

Other Geochemical–Gravity Correlations: The uranium, rubidium, and fluorine data sets were chosen for correlation with the gravity data as they showed the most significant variation in their spatial distribution. Other elements did not vary as much geographically or in range.

Distribution maps for the individual elements and for the element–gravity correlation scores were prepared. The element–gravity correlation maps showed little difference from the element-concentration maps, indicating that the density of the granite is controlled mainly by the SiO_2 composition as demonstrated earlier. Tuach *et al.* (1986), have demonstrated that there is no significant correlation between the Rb, U, F and Si, hence the lack of significant correlation between these elements and the gravity data is not unexpected. Because these data exhibit low Pearson correlation coefficients, which are, at best, marginally significant, the element and correlation distribution maps have not been included in this report. Nevertheless, the technique is a useful one to apply and assess when investigating an area.

The element concentration and correlation data indicate that the regions of granite of most interest in explaining the processes, whereby the chemical elements are transported are the boundaries between the Rencontre Lake Granite and Hungry Grove Granite and between Sage Pond Granite and the Hungry Grove Granite. These areas are also the areas where the deepest lobes of granite occur.

SUMMARY

The geophysical and physical property data suggest that the Ackley intrusive suite is significantly different from the surrounding country rocks in its physical properties and gravity signatures. Both the gravity and magnetic data, when interpreted together, outline the areal extent of the granites and demonstrate the existence of the Dover–Hermitage Bay Fault as a fundamental feature beneath and within the granites. The data also suggest the existence of parallel northwest–southeast-trending lineaments in the basement beneath the granite. Gravity inversion and magnetic modelling results demonstrate that lineaments are steep, subsurface boundaries, which are interpreted as faults, along which significant downward vertical motion of blocks of Avalon material occurred just prior to, or contemporaneous with, the emplacement of the Ackley intrusive suite rocks. This suggests a process of megastoping into a magma chamber formed by frictional heating from motions on the Dover–Hermitage Bay Fault of blocks having typical widths of the order of 10 km (Figure 14).

The patterns of granite thickness (Figures 8, 9 and 10) show a strong degree of correlation with these linear features as well, indicating that the possible movement on the features was probably concurrent with the intrusion of the granite. This is also supported by the strong correlation of the geochemical trends with the lineament-bounded blocks.

The correlation of the deepest lobes with the lowest density suggests that the low density magma migrated upward along conduits located near the boundaries of the Ackley intrusive suite with the surrounding country rock. The gravity methods were unable to resolve the slope of the interface between the Avalon Zone rocks and Ackley intrusive suite in the south because of an inferred low density contrast across the boundary, but the symmetry of the magnetics suggests that the boundary is near vertical. The various inversion methods taken together, imply that there must be several kilometres of granite located beneath the volcanic rocks of the Avalon Zone, ir. the area between the Rencontre Lake and Sage Pond granites, and that the Sage Pond Granite may continue beneath the volcanic rocks for several kilometres south of its outcrop boundary. These conclusions are consistent with the presence of granitic dykes and fluorite veins in these areas.

CONCLUSIONS

The study of the combined geophysical, geochemical and geological data for the Ackley intrusive suite and the surrounding country rocks, has demonstrated the power of an integrated approach. In particular, the following contributions to the understanding of the area were made:

(1) the bottom morphology of the granites was determined by gravity inversion methods,

(2) the presence of Avalon Zone mafic rocks beneath the granite south of the Dover–Hermitage Bay Fault was interpreted from magnetic data, which also corroborate the depths to the bottom of the granite determined from gravity, and

(3) distinctive, northwest–southeast lineations were identified; these are interpreted to be faults in the basement beneath the granite and are considered to be conduits for emplacement of granitic magma by megablock stoping of Avalon Zone material along these faults.

THE NORTHEASTERN GANDER ZONE

INTRODUCTION

The study area (Figure 15), is situated in north-central Newfoundland and is bounded to the south by the Trans Canada Highway (Route 1), to the west by the Gander–Carmanville road (Route 330), on the north by Hamilton Sound, and to the east by the Gambo–Cape Freels road (Route 320). Access to the area is by the existing network of highways and bush roads and by boat and helicopter.

The objective of the field work was to provide additional detailed geophysical data, to determine the extent of a belt of rocks having anomalous magnetic and gravity signatures, identified earlier by Miller and Weir (1982). Additional gravity data were collected to supplement those reported by Weaver (1968), Weir (1971), Miller and Weir (1982), and Miller (1983). The new gravity data were collected at 238 localities during the 1985 field season (Miller, 1985). During the interpretation phase, the existing Geological Survey of Canada 1:63360 aeromagnetic maps for the area were processed, filtered and used in conjunction with the gravity data in developing models of the geology.

GEOLOGICAL REVIEW

The geology of the southern, western and eastern areas has been systematically mapped on both reconnaissance and detail scales (Jenness, 1953a, b; Kennedy and McGonigal, 1972; Blackwood, 1977, 1978, 1979a,b, 1980, 1981b; Jayasinghe, 1978). Additional detailed mapping of specific areas has been reported by Pajari and Currie (1978), Pajari *et al.* (1979), and Wonderley and Neuman (1984). The central section consisting of the Weir's Pond (2E/1) map area was mapped on a 1:50,000 scale (O'Neill, 1987). Figure 15 is a

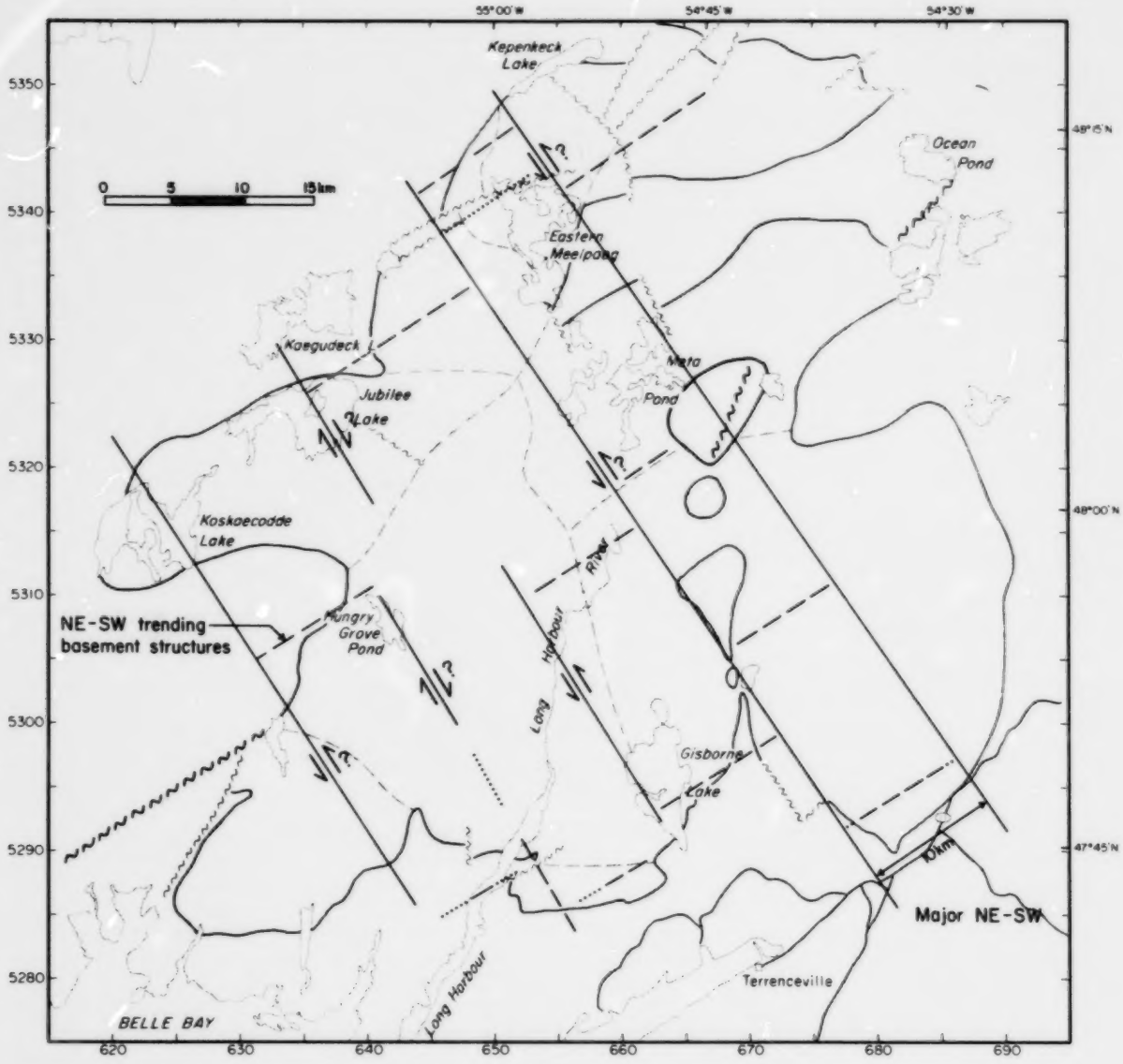

Figure 14. *Parallel lineament features in the Ackley study area.*

composite geological map of the mineral occurrence maps for the Botwood (2E), Gander Lake (2D), and Wesleyville (2C) map areas. The geology was derived from the reports mentioned above and from reports compiled by Andrews (1980), Blackwood (1981a, b), and Blackwood *et al.* (1983) respectively.

The area contains part of three major zones of the Appalachians, the Dunnage, Gander and Avalon (Williams and Hatcher, 1983). The Dunnage Zone contains a typical oceanic crustal sequence overlain by volcanogenic sediments and island-arc sequences, and is found west of the Gander River Ultrabasic Belt (GRUB line); it is represented by the clastic sediments of the Davidsville Group in the south near the Trans Canada Highway (Blackwood, 1982). In the north, the typical Davidsville Group rocks are overlain by the transported Carmanville mélange, which contains the whole oceanic crustal sequence (Pajari *et al.*, 1979). The Dunnage and Gander zones, are separated by the GRUB line, which is marked at surface by discontinuous outcrops of ultramafic rocks, although some authors have noted that the aeromagnetic data suggest that there must be ultramafic rocks, which are probably continuous at shallow depths (Blackwood, 1982; Miller and Weir, 1982).

East of the GRUB line, throughout the area, except for the extreme north, the Gander Group sediments are found in either fault contact or in inferred fault contact with the

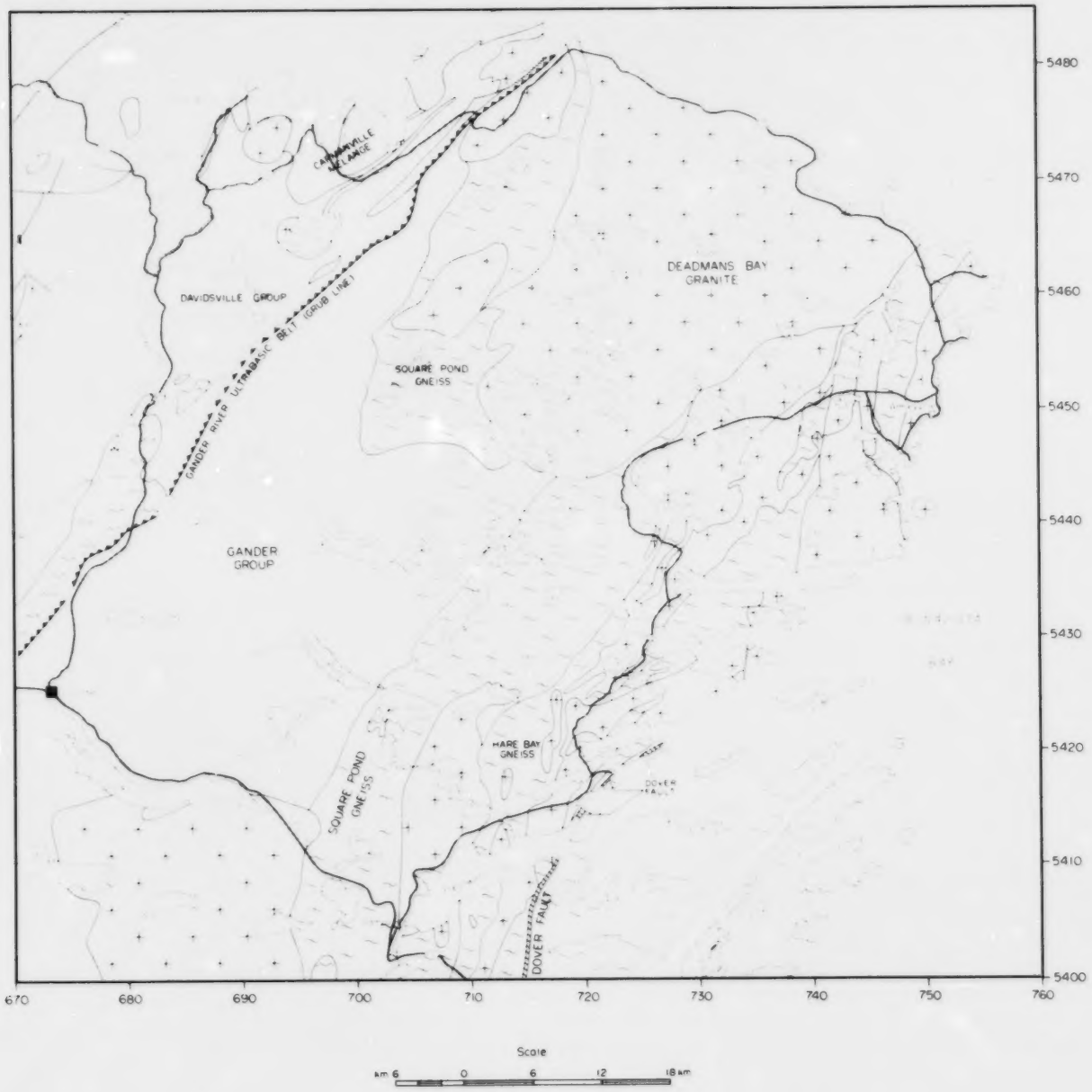

Figure 15. *General geology of northeastern Gander Zone based on Andrews (1980), Blackwood et al. (1983) and Blackwood (1981a, b). Coordinates are UTM Zone 21, and in kilometres; map scale 1:250,000; same coordinates and scale used in Figures 16 to 22.* ~ *Square Pond Gneiss, Hare Bay Gneiss;* + *various granites;* Blank area, *Gander Group and Davidsville Group metasediments.*

GRUB line ultramafics or the Davidsville Group clastics (Blackwood, 1982; Pajari and Currie, 1978). In general, the Gander Group rocks are polydeformed and metamorphosed, although Blackwood (1978) and Wonderly and Neuman (1984) report the presence of relatively fresh pillow lavas in the vicinity of Indian Bay Big Pond in an interpreted thrust sheet (Wonderly and Neuman, 1984). The Gander Group immediately south of Gander Lake is intruded by a medium to coarse grained, megacrystic biotite granite assumed to be Devonian in age. A foliated, medium grained, muscovite–biotite granite, the Ragged Harbour granite, intrudes the northern boundary between the Gander Group and the GRUB line.

The Gander Group is underlain by the Square Pond Gneiss, which is in turn underlain by the Hare Bay Gneiss (Blackwood, 1977). The Square Pond Gneiss, considered by Blackwood (1982) to be the metamorphosed equivalent of the Gander Group, is found in a 10-km-wide band immediately east of the Gander Group. Its outcrop area to the north is offset by approximately 15 km west of the exposure in the southern half of the map area. It is intruded by the Ocean Pond granite and a small similar granite in its western outcrop area. In the east, several small diorites and gabbros are mapped in the Square Pond Gneiss belt. The largest intrusion in the belt is the Deadmans Bay Granite, a Devonian massive, medium to coarse grained, feldspar megacrystic, biotite granite.

The Hare Bay Gneiss forms a continuous band along the eastern margin of the Gander Zone. It is intruded by several granites of various ages. In the southeastern corner, it is in fault contact with the Avalon Zone rocks to the east. This fault, the Dover Fault, follows an arcuate path to the northeast and disappears beneath the waters of Bonavista Bay.

GEOPHYSICAL REVIEW

The area has been included in numerous regional and Appalachian scale geophysical interpretations (Weaver, 1967; Miller, 1977; Haworth, 1977, 1981; Jacobi and Kristoffersen, 1976, 1981; Haworth and Jacobi, 1983), but has been the subject of only one specific interpretation (Miller and Weir, 1982). Numerous local exploration surveys have been conducted primarily in the western section of the area, but these have been of limited extent. The target for these surveys has been the mineralization associated with the GRUB line.

The regional and orogenic interpretations have identified the Gander Zone as having geophysical signatures distinct from those of the adjacent Dunnage and Avalon zones (Miller, 1977; Jacobi and Kristoffersen, 1976; Haworth and Miller, 1982). The main distinguishing feature of the Gander Zone is its primarily negative gravity and magnetic anomalies, although the magnetic anomalies do become positive, locally. This combination of gravity and magnetic signatures has led to the affirmation, both on geophysical and geological grounds, that the GRUB line marked the easternmost location of Dunnage Zone rocks. This view has been tempered by the interpretation of the deep crustal reflection seismic data (Keen *et al.*, 1986), the reinterpretation of the refraction data (Mitchelmore, 1985), and the interpretation of the gravity and magnetic data (Miller and Weir, 1982). The seismic data suggest the only major crustal discontinuity in the region occurs at the Dover Fault, and indeed one can discern the presence of apparent thrust sheets east of the GRUB line on the reflection data. There is also geomagnetic depth sounding data to suggest the presence of a major electrical conductivity contrast across the Gander–Avalon boundary (Cochrane and Wright, 1977; Pal, 1982).

The interpretation of Miller and Weir (1982) focussed on the gravity and magnetic data of the western section of the present study area. They presented a model for the juxtaposition of the Carmanville mélange and the GRUB line in the north and deduced the presence of rocks similar to those along the GRUB line beneath the granite, adjoining Gander Lake in the south. They identified a broad band of positive aeromagnetic anomalies in the centre of the Gander Group, which they termed the Ocean Pond anomaly. Their modelling of this anomaly suggested that it was related to anomalous mafic to ultramafic material deduced to underlie the granite at Gander Lake and to extend from the Trans Canada Highway in the south, to the Ragged Harbour granite in the north. At the time of this interpretation, the initial results from geochemical surveys (Butler and Davenport, 1981) became available, and the correlation of the geophysical and geochemical data sets suggested that a further examination of the area was desirable, especially after Wonderley and Neuman (1984) reported the presence of pillow lavas in an interpreted thrust sheet at Indian Bay Big Pond, at coordinates 710E,5438N of Figure 15.

During the 1983 field season, three gravity traverses were conducted across the southern portion of the area to determine if the proposed Indian Bay Big Pond thrust sheet had a significant signature and to examine the gravity signature associated with the Ocean Pond magnetic anomaly belt (Butler *et al.*, 1984). The positive results of the initial project led to the present project, in which a systematic gravity survey was conducted over the northeastern section of the Gander Zone.

PRESENT STUDY

The field work associated with the present study concentrated on the collection of gravity data in the interior portion of the Gander Zone, north of the Trans Canada Highway and west of the Gambo–Cape Freels road. Stations were occupied at 2.5-km spacing along the highways and at 1-km spacing along major bush roads in the vicinity of Indian Bay Big Pond and along the shores of other ponds in the area. Helicopter traverses at 5-km spacing were conducted in the northeastern part of the area. All gravity readings were obtained with a Lacoste and Romberg land G meter and elevations were determined by barometric altimetry. Existing gravity base stations at Gander, Wesleyville, and Carmanville (Appendix 1) were utilized for gravity control and new control stations were established at Trinity and at the intersection of the main highway network (Route 320) and the woods-road network in the eastern region. Altimeter control stations were established at the gravity control stations by rod and level surveying, from the existing tidewater line and corrected for tidal effects using tide tables. The control station at Trinity was located at a Newfoundland Crown Lands Geodetic control point, for which the elevation was known; the station at the woods-road intersection was tied to this control point by repetitive barometric surveying which established its elevation to better than 0.5 m.

All gravity data collected in the 1985 survey were reduced to Bouguer anomalies using the 1967 International Gravity Formula, the IGSN71 base system, to which the control stations are tied via the control stations of the Canadian

National gravity network, using a crustal density of 2.67 g cm^{-3}, using the formulae of Appendix 1. No corrections were made for earth-tide effects or for terrain effects, as both are considered to be minimal in the area. The earlier gravity data from Butler *et al.* (1984) and Miller and Weir (1982) were included in the file without further adjustment. The data from Weir (1971) and Weaver (1968) were reduced by 6.2 mGal to accommodate the change to the IGSN71 system. The overall accuracy of the Bouguer anomalies throughout the study area is considered to be +/−0.5 mGal based upon the elevation, gravity reading, and position uncertainties. A complete listing of the principal facts for all 539 gravity stations used in the compilation and interpretation is given in Miller (1985). The resulting Bouguer anomaly map with station localities posted is presented in Figure 16.

The aeromagnetic maps for the study area had been digitized and filtered as part of the Miller and Weir (1982) study. However, all of these data had not been reduced to the same datum. By considering the match between the proton precession data and the fluxgate data along the boundaries between the appropriate map sheets, a regression equation was determined to correct the fluxgate data to equivalent total field data. The IGRF 1965.0 was then removed from the digitized data and the data filtered using a 25 point averaging filter, to produce a magnetic data set having 4.25-km spacing, similar to that of the gravity data (Miller and Weir, 1982; Miller, 1986). The processing sequence is presented in Appendix 2. The resulting total field magnetic anomaly is presented in Figure 17.

The geochemical data used in the study were obtained from the data file for the area (Butler and Davenport, 1981; Butler *et al.*, 1984). For the present study only the copper, lead, zinc, cobalt, nickel, molybdenum, fluorine, and uranium data were considered, and concentration maps for these elements were plotted to determine areas of significant correlation of the elements with the geophysical data. Only the uranium and nickel maps are presented here since these exhibit the most compelling correlations with the areas of interpreted granitic and ultramafic rocks respectively (Figures 18 and 19).

All the maps for the study area were contoured using the SURFII package (Sampson, 1978) with an interpolation grid interval of 4 km and only a single smoothing. This interpolation interval is consistent with the aeromagnetic, gravity, and geochemical data spacing, as all data were derived from data sets having between 500−700 data points over the same geographical area. Thus the wavelength of the features emphasized on all the data sets is approximately the same. Equally spaced contour intervals were used for the geophysical data. The geochemical data are contoured using levels determined from the statistical distribution for the particular element.

QUALITATIVE INTERPRETATION

In the west, the Bouguer anomaly map (Figure 16) is dominated by a northeasterly trending region of positive Bouguer anomalies that correlate with the location of the previously interpreted GRUB line and Carmanville mélange anomalies (Miller and Weir, 1982). East of this, the anomalies are predominantly negative except for a northeasterly trending belt from 700E,5420N to 710E,5450N. The eastern margin of this belt, termed the Indian Bay Big Pond Thrust belt (proposed new name), coincides with the thrust belt interpreted by Wonderly and Neuman (1984) at 713E,5440N and the nature of the gravity gradient is typical of the pattern to be found over the edge of a shallow, west-dipping thrust sheet, which abruptly terminates at that location. The remainder of the area is typified by negative Bouguer anomalies, which in general correlate with the major granites, although there is a hint of a belt of negative anomalies immediately east of the GRUB line in the area of the Ocean Pond magnetic anomaly at 700E,5440N, identified by Miller and Weir (1982).

In order to examine the more subtle features of the gravity field of the area and to remove the dominant effect of the strong regional anomaly associated with the GRUB line, a regional trend was removed using a third order polynomial trend surface, determined from the data using the program of Whitten (1971). The resulting residual gravity map derived by subtracting the regional trend value at each locality from the Bouguer anomaly at that point is presented in Figure 20. It is apparent from this map that the belt of negative anomalies immediately east of the GRUB line can be continued south, to link with a set of negative residuals immediately north of the major granite south of Gander Lake (Figure 15). The residual gravity low centred at 704E,5460N, coincides with the outcrop of the Ocean Pond granite and the west lobe of the low to the north−northeast of this occurs over the Ragged Harbour granite. This correlation of the residual gravity lows in this belt with existing granites suggests that similar granites are located beneath the surface throughout this belt. Granites exist in a similar position relative to the GRUB line south of the study area (Blackwood, 1982).

The second major feature, which is emphasized by the residual map, is the Indian Bay Big Pond Thrust belt. The residual data suggest that the positive gravity anomalies associated with it may continue northeastward across the Deadmans Bay Granite. The residual anomaly map also indicates that there may be two northwest−southeast breaks running from 680E,5480N to 720E,5445N and from 670E,5440N to 700E,5410N, which truncate the gravity residual high. The residual gravity low, east of the GRUB line is noticeably less pronounced between these two trends.

The magnetic total-field anomaly map (Figure 17), exhibits the same general northeasterly trends seen on the gravity maps and to a lesser degree the northwest−southeast trends may be discerned. Two interesting correlations between the two maps are those of the gravity low from east of the GRUB line with a zone of positive magnetic anomalies, the Ocean Pond anomaly of Miller and Weir (1982), and the Indian Bay Big Pond Thrust belt gravity anomaly with a zone of negative magnetic anomalies. Immediately to the east of this latter zone is a zone of positive anomalies situated over

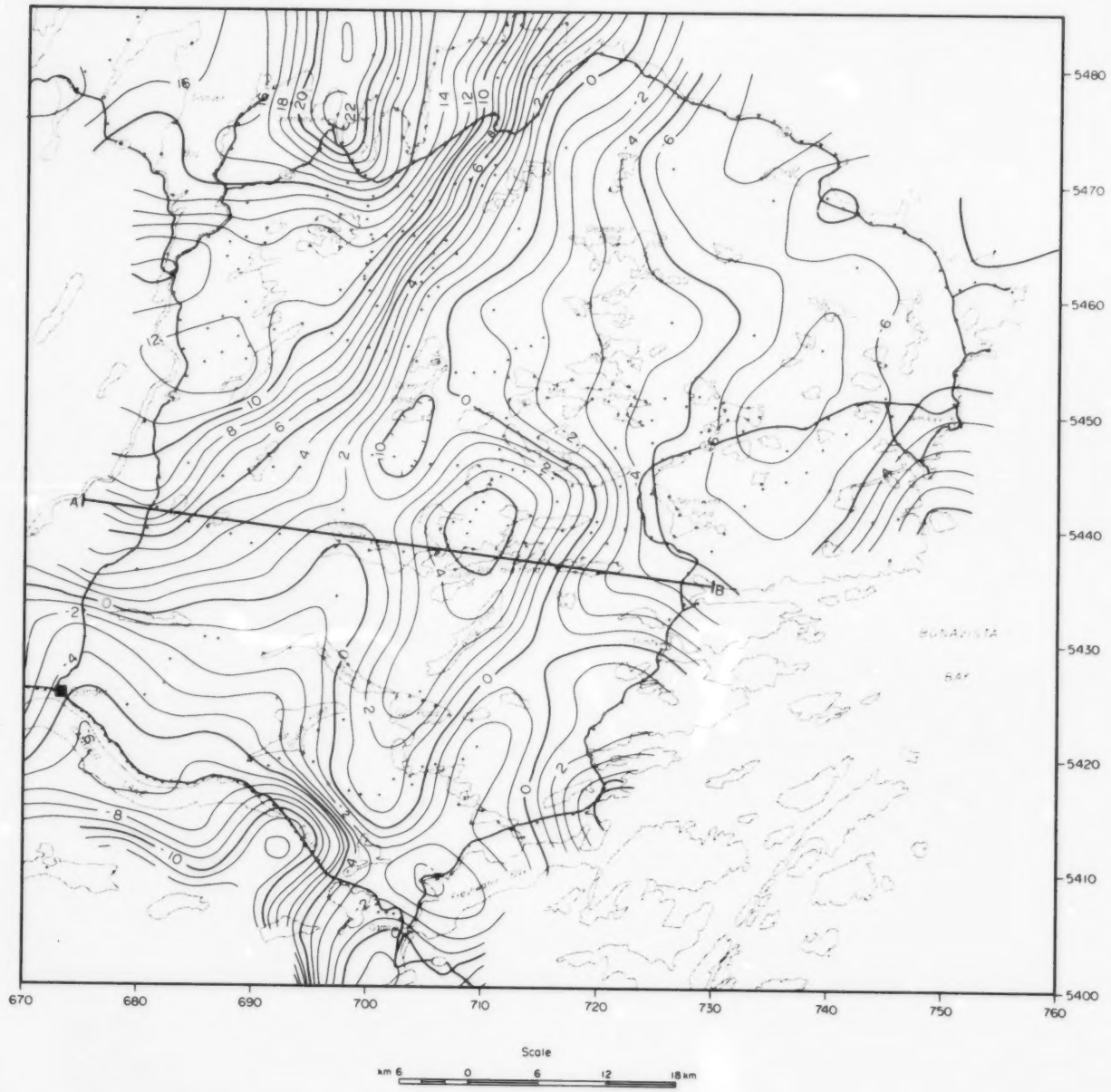

Figure 16. *Bouguer anomaly map for the northeastern Gander Zone area; + denotes gravity station location; contour interval 1 mGal. AB, interpreted profile.*

the Square Pond Gneiss belt, a feature noted by Blackwood (1977).

The more subtle trends in the magnetic data are difficult to discern on the total field anomaly magnetic map, so in order to enhance them, a second derivative magnetic map was produced from the aeromagnetic data. This was accomplished by interpolating the data onto a regular 4-km grid using the SURFII package and then applying a simple second vertical derivative filter (Henderson and Zeitz, 1967; Miller, 1976), which accentuates the boundaries between various magnetic units and enables trends to be more readily examined (see Appendix 2 for details of the procedure). The resulting map (Figure 21) demonstrates the more complex nature of the

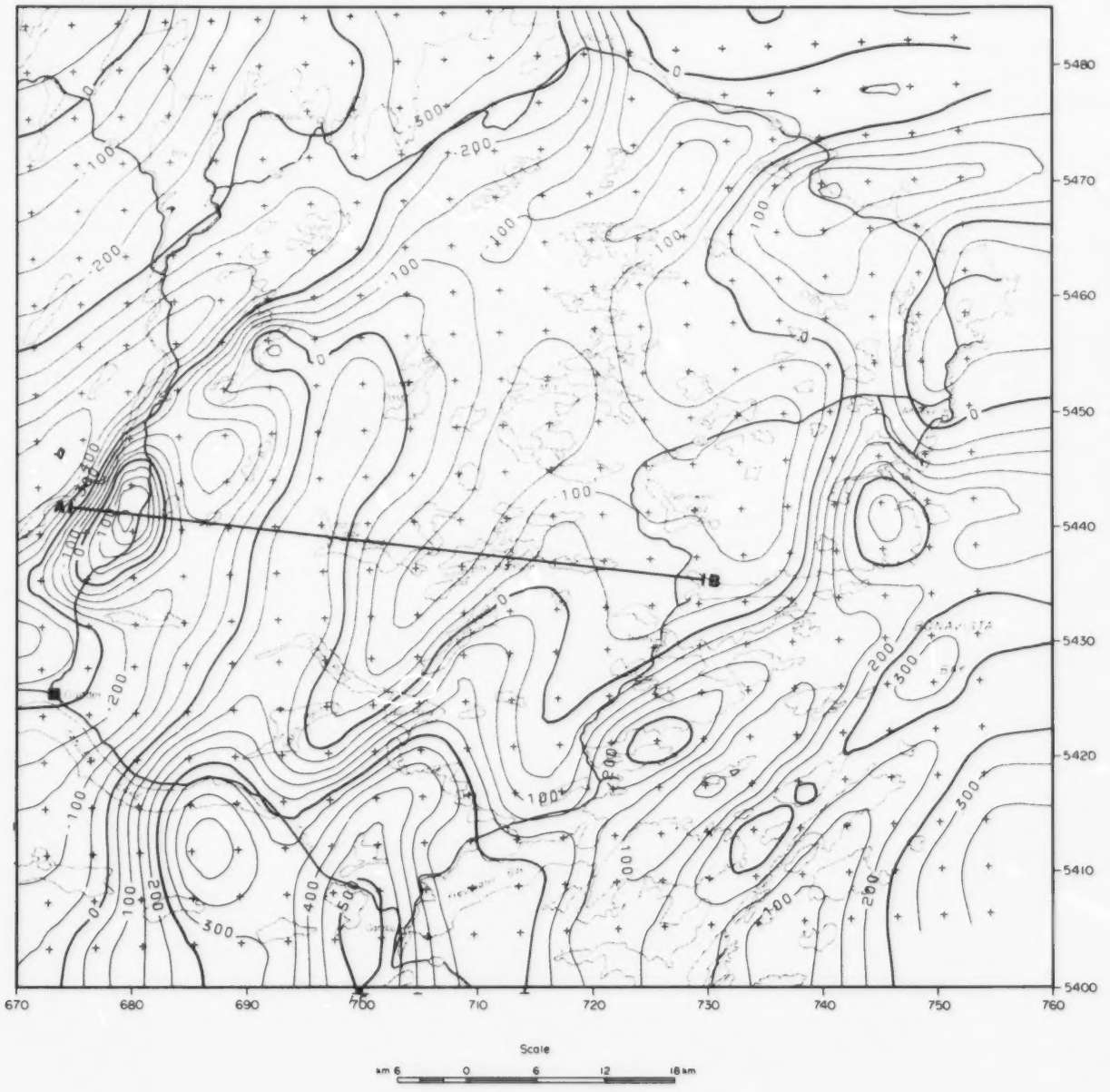

Figure 17. *Total-field magnetic anomaly map for the northeastern Gander Zone area: + denotes location of averaged data point; contour interval 50 nT; magnetic anomalies are relative to IGRF 1965.0. AB, interpreted profile.*

magnetic data especially beneath the Deadmans Bay Granite. The northwest–southeast breaks recognized on the residual gravity data are apparent on the second-derivative map. It is apparent that a major truncation of the second derivative trends along a northeast-trending line and occurring at 690E,5460N, where the geological mapping indicates that no ultramafics are present at surface, but where magnetic anomalies suggest they may exist beneath the surface (Pajari *et al.*, 1979). Also, in this area, the magnetic trends from the Ocean Pond Anomaly belt on both the magnetic anomaly and second-derivative magnetic maps intersect the GRUB line trends obliquely. The magnetic low coincident with the Indian Bay Big Pond Thrust belt positive gravity anomaly and the magnetic high immediately east of it, both show up as strong northeast-trending features perturbed to the south and north by the northwest–southeast breaks mentioned earlier,

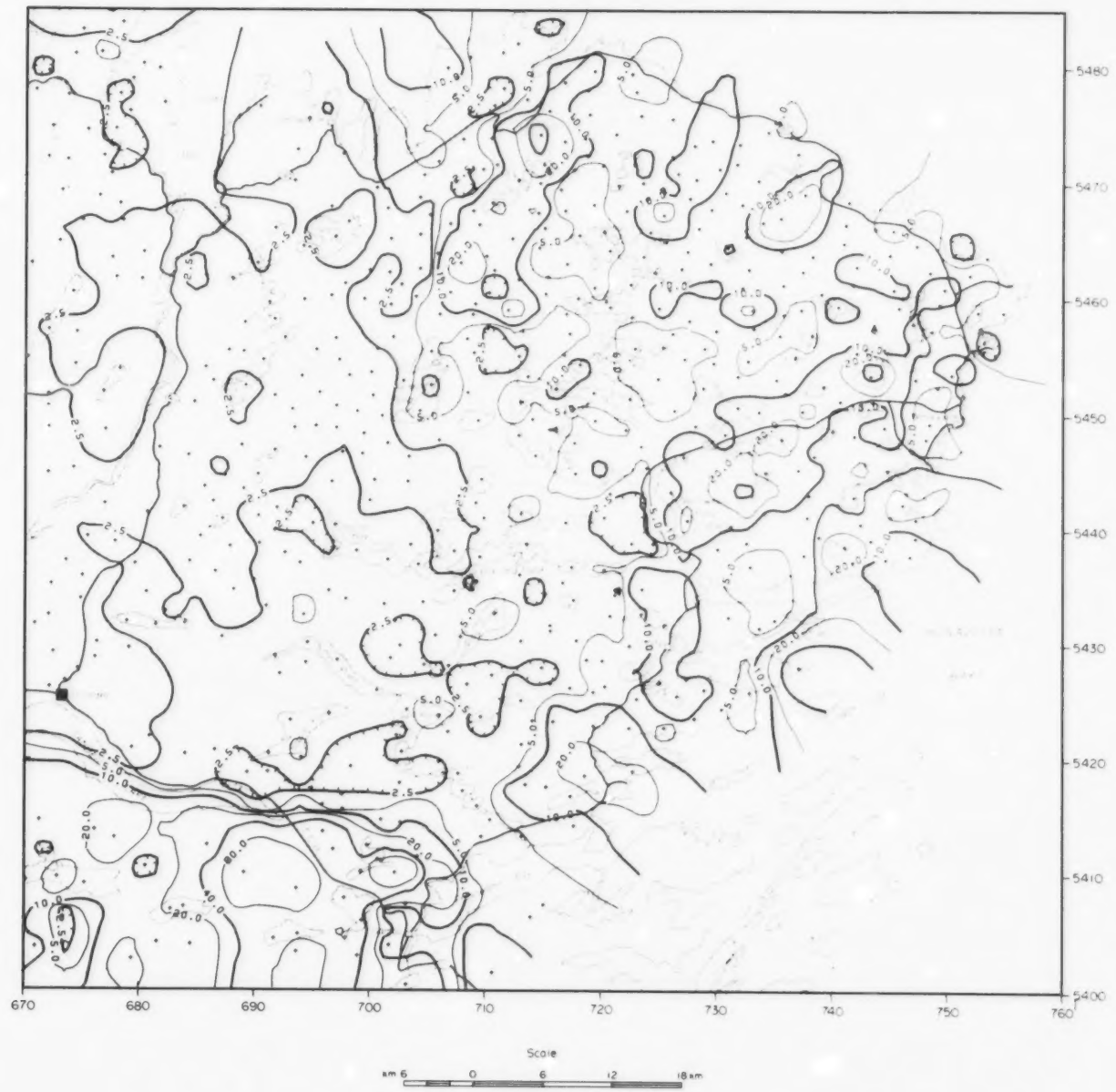

Figure 18. *Uranium anomaly map for the northeastern Gander Zone area; + denotes geochemical sampling location; anomalies are in ppm; variable contour interval chosen on the basis of distribution statistics.*

although there is evidence that a magnetic low continues beneath the Deadmans Bay Granite where its pattern is more complicated. This northern low may perhaps then be a different feature, which fortuitously appears at this position.

The magnetic trends associated with the Avalon Zone and the Dover Fault are quite pronounced in the southeast corner of the area, occurring as alternating bands of positive and negative magnetic anomalies typical of the Avalon (Haworth and Lefort, 1979; Miller *et al.*, 1985). The more northerly of the northwest–southeast breaks appears to truncate the Dover Fault or at least coincides in a change in the trend of the fault in the vicinity of 750E,5435N, an area where the geological mapping indicates it strikes out to sea

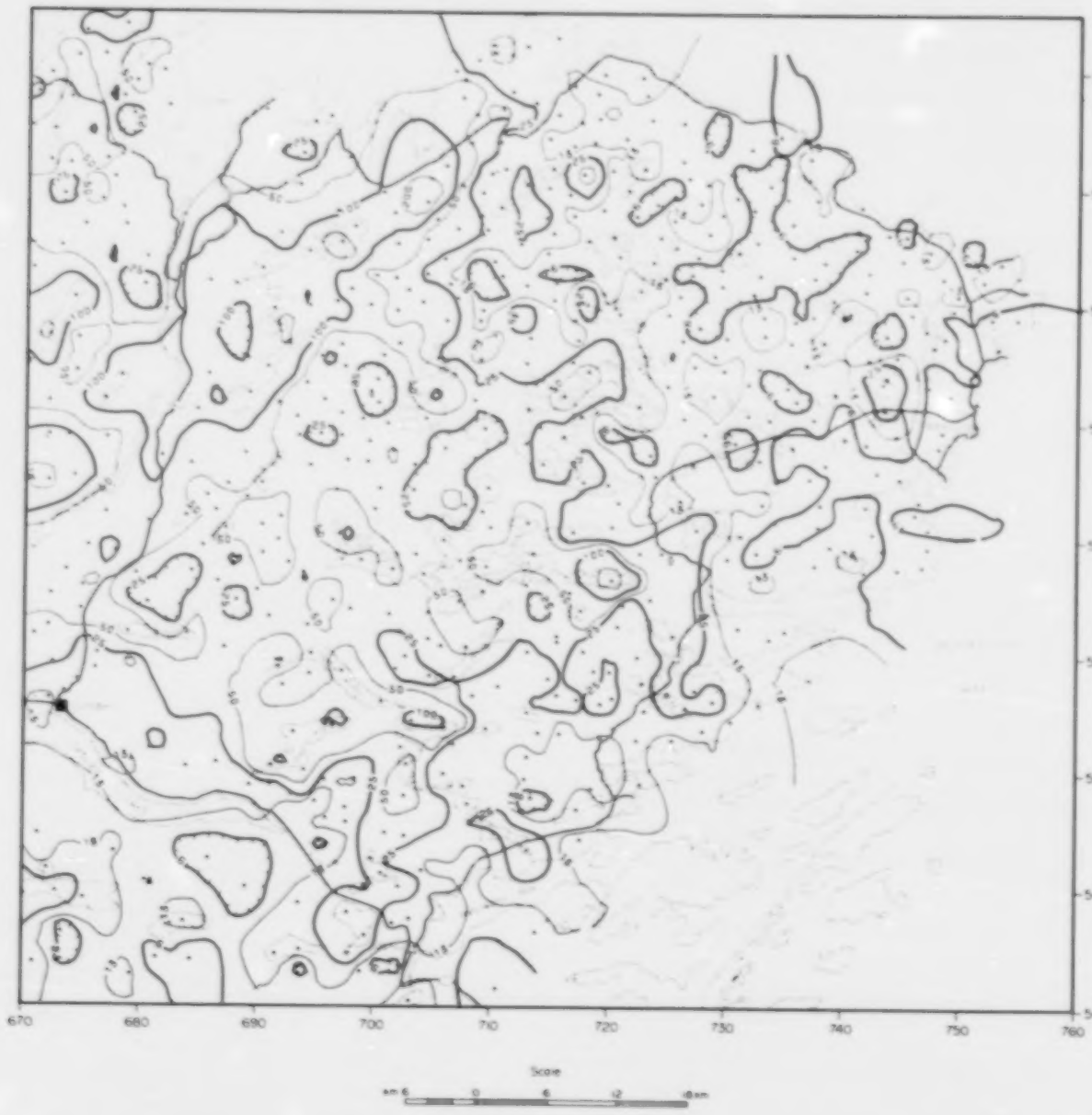

Figure 19. *Nickel anomaly map for the northeastern Gander Zone area. Anomalies in ppm. Sampling sites same as Figure 18. Variable contour interval chosen on the basis of distribution statistics.*

beneath Bonavista Bay. The southern break intersects the fault at 717E,5410N, where there is a visible change in the strike of the fault.

All of these data suggest that the area between the two northwest–southeast breaks is different from the area south of Gander Lake and that there may be at least two areas beneath the northeast Gander Zone where mafic and ultramafic rocks may exist in the near subsurface east of the GRUB line. In order to examine the composition of these subsurface rocks, the geochemical data for the area were plotted on the same scale. The most striking correlations, which confirm the interpretation of the Indian Bay Big Pond belt as a thrust of Dunnage Zone material to the nearsurface, are provided in the correlation of elevated cobalt, nickel, lead, and zinc values with the east side of the thrust sheet in the

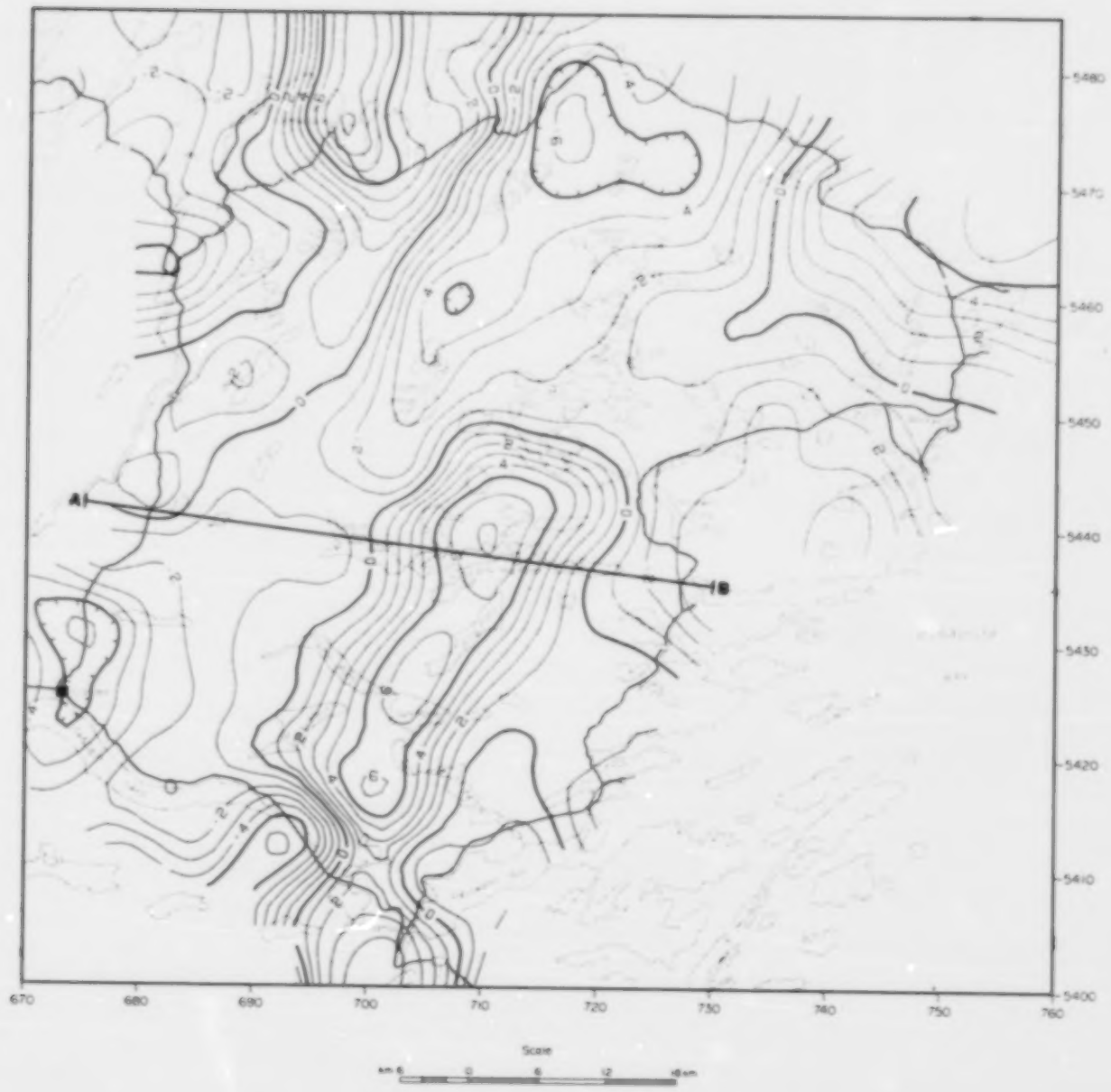

Figure 20. *Residual-gravity anomaly map for the northeastern Gander Zone area; contour interval 1 mGal. AB, interpreted profile.*

area mapped by Wonderley and Neuman (1984). When the compilation map, Figure 22, is compared with the nickel anomaly map, Figure 19, it is obvious that the area bounded by the two northwest trend lineations and the eastern boundary of the Indian Bay Big Pond belt is the same as the area bounded on the north, south and east by the 25 ppm nickel contour. The coincidence of these features confirms the anomalous nature of the region inside these boundaries and suggests that elsewhere in the Gander Zone, the nickel distribution maps could be used in conjunction with the existing aeromagnetic maps to outline anomalous areas. A similar, less pronounced anomaly in the same elements occurs at the eastern edge of the Ocean Pond Anomaly belt.

The absence of significant uranium anomalies in the Deadmans Bay Granite, and the occurrence of significant

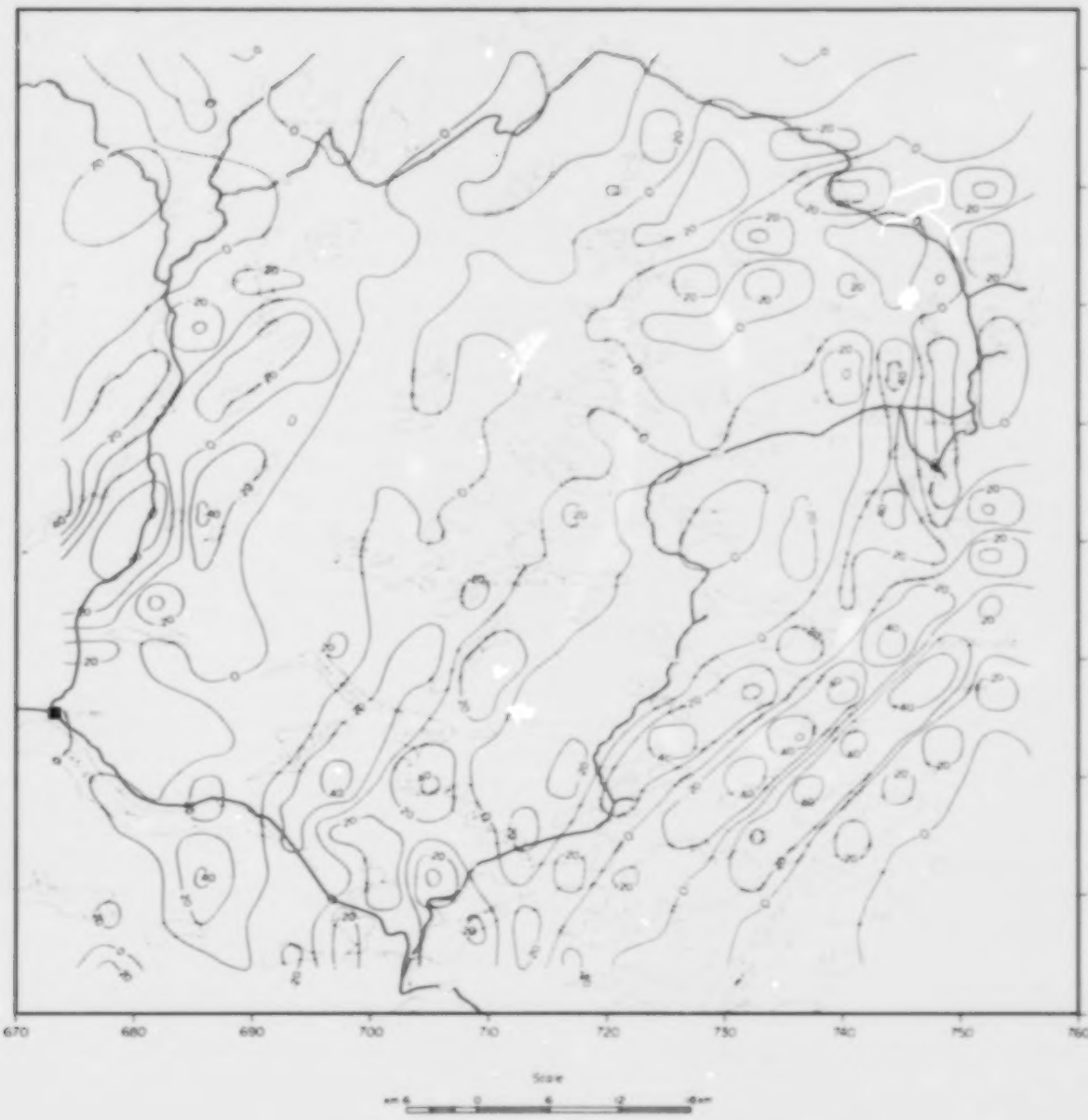

Figure 21. *Magnetic second-derivative map; contour interval 20 nT/km².*

cobalt anomalies along the western margin of the extension of the Indian Bay Big Pond Thrust belt through the pluton, reinforces the interpretation that the Deadmans Bay Granite is underlain by more mafic material. Uranium anomalies are noticeably absent in the Ocean Pond anomaly belt between the outcrop of the major granite south of Gander Lake and the area of the Ocean Pond granite. This raises questions about the presence of granitic rocks suggested earlier based upon gravity and magnetic data; it could imply that any granite in this area may exist in the deeper subsurface preventing the uranium from reaching the surface (J. Tod, personal communication, 1986). The overburden thickness throughout the area is not known accurately, but limited trenching and investigation of the thickness suggests it is less than 5 m (D. Vanderveer, personal communication, 1986).

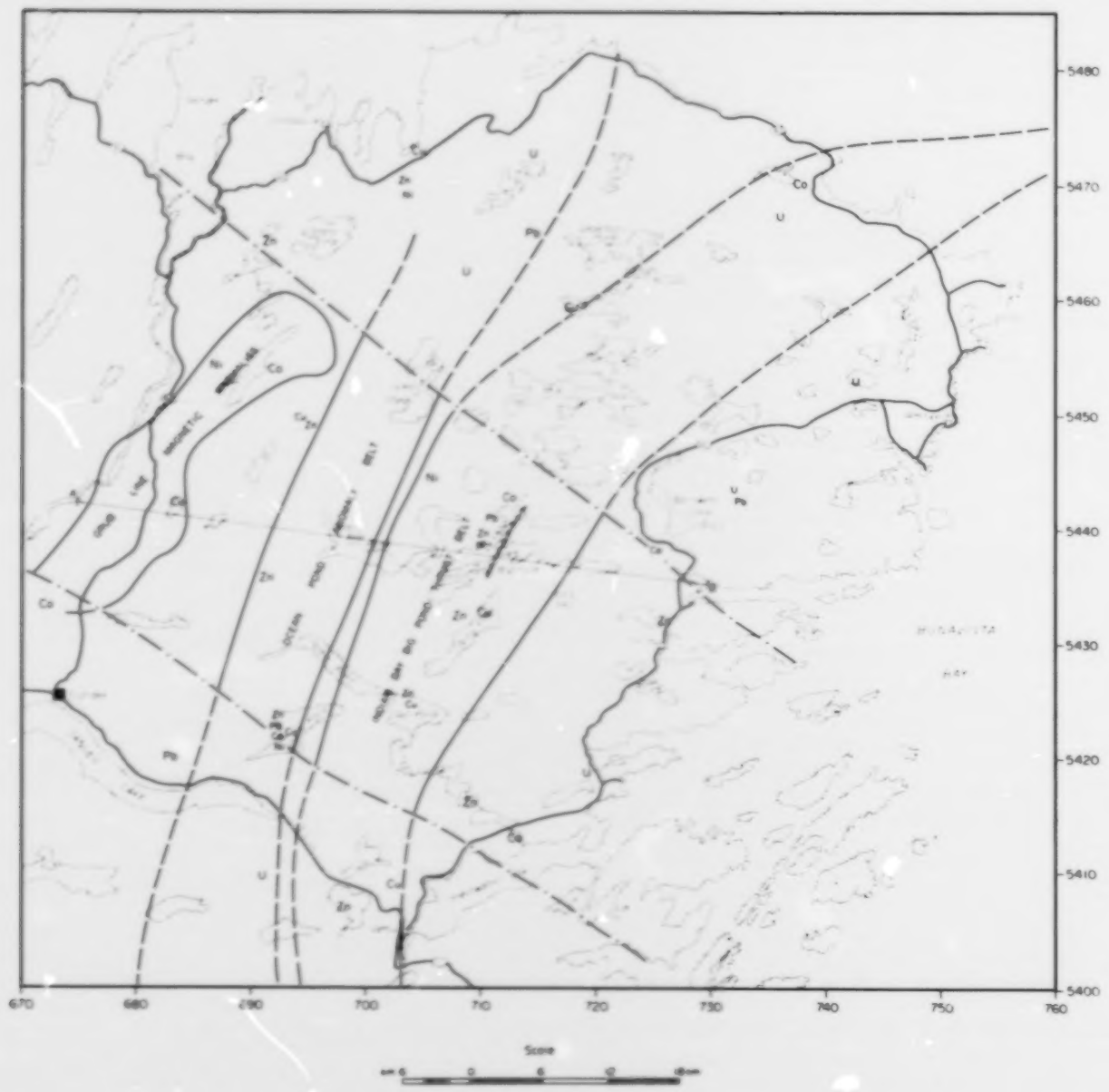

Figure 22. *Compilation map for the northeastern Gander Zone geology, geophysics and geochemistry.* Dash-dot lines *indicate NW–SE breaks,* solid lines *delineate interpreted belts discussed in text.*

QUANTITATIVE INTERPRETATION

The qualitative interpretation discussed above can be substantiated by quantitative modelling of the gravity and magnetic data, using standard 2-D modelling techniques as the strike length of the various features is considerably greater than their profile width. In order to examine a typical profile across both of the anomaly belts in the Gander Zone east of the GRUB line, and to ensure that the selected observed data points were close to, or on, the selected profile, the transect shown on Figures 15, 16, 17 and 20 was chosen. Only the magnetics and the residual gravity were modelled in order to emphasize the features immediately east of the GRUB line.

The modelling (Figure 23) illustrates the necessity of including granitic material immediately east of the GRUB line, although neither the geophysical modelling of this study nor more detailed modelling (J. Tod, personal communication, 1986) can resolve the question of whether to place this material at surface or at depth. The fundamental point that emerges from these models, is that such material must exist in the Gander Zone at this location, and that it must have mafic to ultramafic material associated with it in order to explain the magnetic anomalies and the nickel and cobalt anomalies. The physical properties used in modelling these features are typical values for the rocks involved (Miller and Weir, 1982), as no extensive rock collection for the area was available to determine the properties.

The quantitative interpretation of the Indian Bay Big Pond Thrust belt presents more problems as the gravity high correlates with the magnetic low. This correlation, the location of a magnetic high on the very eastern edge of the belt, and the steep gravity gradient associated with the mapped exposure of the thrust, all suggest that the causative bodies dip westward and that part of the anomalies are caused by an eastern portion of the source that does not outcrop. A small but increasingly negative eastward magnetic gradient effect from the Dover Fault is included in the model to reproduce the regional magnetic level.

SUMMARY

The combined geophysical and geochemical data for the northeastern Gander Zone provide substantial quantitative factual and interpretive evidence for the existence of two belts of mafic to ultramafic rocks in the subsurface. The boundaries of the two anomaly belts as deduced from the combined geophysical and geochemical data are presented in Figure 22, which also presents a summary of the geochemical data. These inferred locations imply that the mafic and ultramafic rocks of the belts then continue beneath the mapped geological features. The implied occurrence of the anomalous rocks beneath the Deadmans Bay Granite suggests that this area warrants further interpretation of the existing data and also detailed mapping of the anomalous area.

The more westerly of the two belts, the Ocean Pond Anomaly belt, is an area in which it is suggested that granites and mafic to ultramafic rocks may exist at depth beneath a cover of Gander Group rocks. The belt terminates against the GRUB line in the northwest but there may be a branch from this anomaly that continues under the Deadmans Bay Granite. The depth to the top of the mafic and ultramafic rocks is probably of the order of about 500 m, although there must be areas where there are shallower slivers to explain the geochemical anomalies. The depth of the top of the granite is not well determined.

The eastern anomaly belt, the Indian Bay Big Pond Thrust belt, is located in the area where there are mapped pillow lavas in an interpreted thrust. The geophysical modelling supports the thrust interpretation and suggests that the thrust continues farther east in the subsurface (Figure 23). No granite is interpreted to exist in this belt between the two northwest–southeast lineaments.

The whole area between the two inferred northwest–southeast breaks (Figure 2) is considered anomalous relative to the surrounding Gander Group rocks and it is suggested that there may have been a southeast offset of the block containing the Indian Bay Big Pond Thrust sheet relative to the similar block to the north. This interpretation is reinforced by the shape of the Square Pond Gneiss belt around the thrust sheet. Further support for the concept of an east-directed thrust belt is evident on the southern boundary of the sheet as delineated by the southern northwest–southeast break. At the location where the break intersects the Dover Fault, there is an eastward turning of the fault. The segment between the two breaks on the GRUB line coincides with the area of the GRUB where the ultramafics are inferred to exist at depth; the processed magnetic data and derivative data indicate that the ultramafics do not reach the surface in that gap.

The nickel distribution map contradicts this by the presence of a strong nickel anomaly. These ultramafics could be the source for the sheets found to the east. The linear nature of the boundaries of this block presents possible evidence of vertical movement on the bounding lineaments. These boundaries should be mapped in detail by a structural geologist to ascertain any field evidence of their form and of any movement on them.

Another major feature emerging from this study is the continuity of the geophysical and some of the geochemical trends across the Deadmans Bay Granite. This warrants further geological and geochemical investigation.

Figure 23: *Gravity, magnetic and geological modelling results for profile AB (Figures 15, 16 and 17). Geological symbols given in Figure 15; v, volcanics, mafic material; ∿, ultramafics; ∫ gneiss belts; +, granite.*

a: Gravity model–residual gravity anomalies in mGal for profile AB denoted by x; anomalies calculated from model denoted by ○.

b: Magnetic model–Magnetic anomalies for profile AB; x denotes observed magnetic anomaly, open circle *denotes anomaly calculated from model shown in Figure 23b;* solid circle *denotes anomaly calculated from model of Figure 23b modified with top of granite at 1.5 km depth, bottom at 5.0 km and all other bodies same as Figure 23b.*

c: Inferred model of subsurface geology.

A

B

FIG. 23a-GRAVITY MODELLING

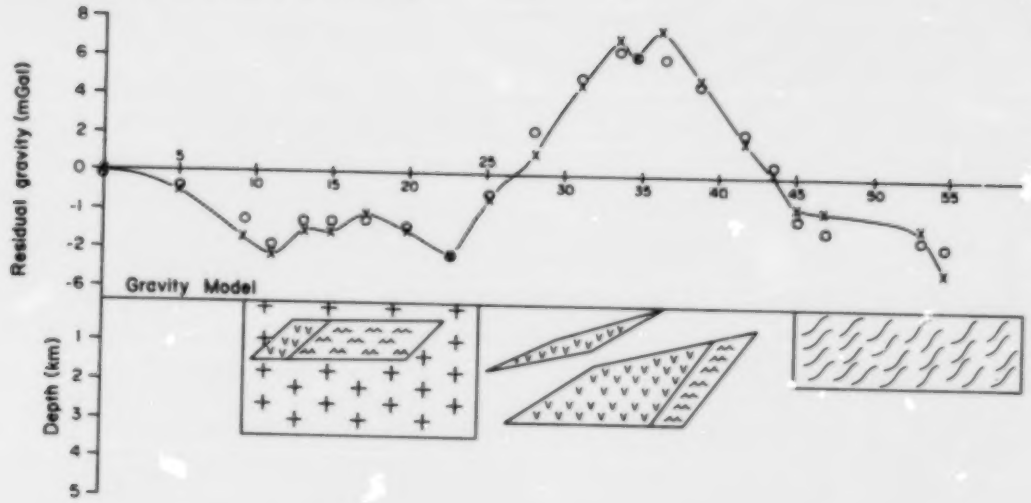

FIG. 23b-MAGNETIC MODELLING

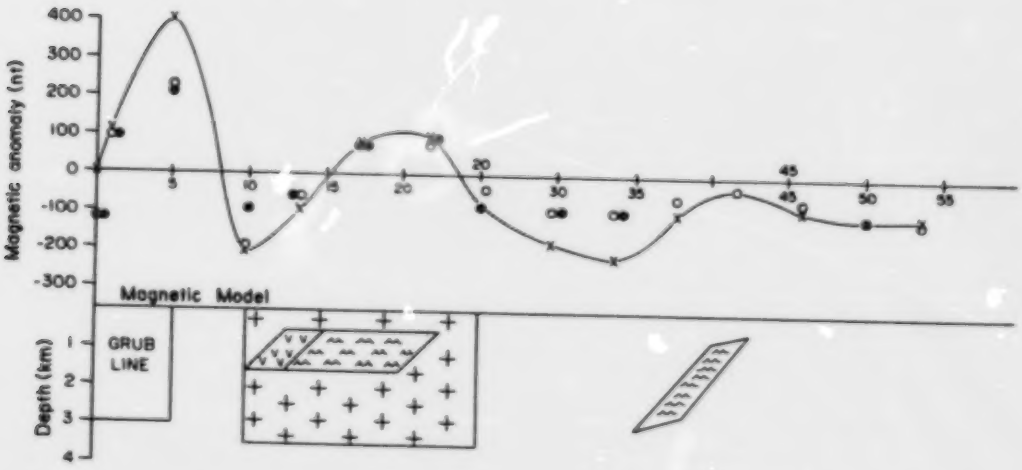

FIG. 23c-GEOLOGICAL MODEL

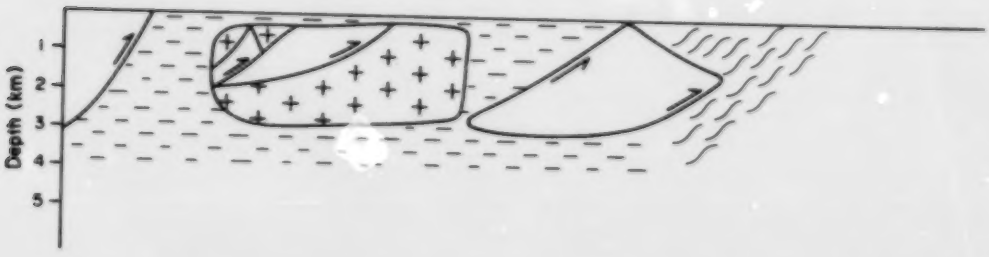

A

B

CONCLUSIONS

The northeastern Gander Zone study demonstrates the efficiency of an integrated interpretation of geophysical, geochemical, and geological data in a complex geological area of limited outcrop. The following conclusions may be drawn from the study:

(1) the GRUB line is not the easternmost limit of Dunnage Zone material in Newfoundland; two other belts, the Ocean Pond belt and the Indian Bay Big Pond Thrust belt also contain Dunnage Zone rocks.

(2) the study area is transected by two northwest–southeast lineations, which appear to cause offsets in the Dover Fault.

GENERAL CONCLUSIONS

The Ackley intrusive suite study clearly illustrates the efficiency of the gravity inversion methods in defining the bottom morphology of a granite terrane, if sufficient information on the density distribution is available. The existence of the magnetic data and the interpreted difference in the source for the gravity and magnetic anomalies suggests that the combined use of these data is a powerful tool to be employed in studying granites in the Canadian Appalachians.

The new spatial correlation methods used to compare the geophysical and geochemical data sets reveal that these methods can provide important cross-correlation information that can lead to inferences about the geological sources of the various parameters. In particular, this method is clearly efficient in demonstrating the presence of major orthogonal trends in the data sets for the Ackley intrusive suite. The computer mapping techniques make it possible to manipulate the large data sets involved, with ease and have contributed to the recognition of the role of the newly identified lineaments as regions of block stoping and subsequent effusion of the granitic melts.

The procedure used in analysing the Gander area data is recommended for further use as it draws upon the expertise from a variety of geoscientific investigations. For future mapping projects in unmapped or poorly understood areas, it is recommended that the geophysicist, geochemist, and project geologist review all the available data for the area well before the field programme is commenced. In this way, the mapping geologist may be informed of the areas of geophysical and geochemical anomalies and be alert to any possible geological manifestations of them in the field.

ACKNOWLEDGMENTS

The author wishes to thank Mr. B. Greene, Assistant Deputy Minister, Geological Survey Branch, Newfoundland Department of Mines, and Dr. P. Davenport, Head, Geochemistry and Geophysics Section, for their encouragement and support of this project, which was undertaken when the author was on sabbatical leave from Memorial University of Newfoundland. J. Tod and J. Tuach read earlier versions of the manuscript and contributed many discussions about the two areas.

R. O'Regan, E. Cumming and T. Gregory collected the 1985 gravity data, L. Houle and C. Cummings assisted the author in acquiring the 1986 data; the 1983 data were collected by S. Peavy, J. Everand and J. Tuach.

REFERENCES

Anderson, F.D.
1965: Belleoram, Newfoundland. Geological Survey of Canada, Map 8-1965.

Anderson, F.D. and Williams, H.
1970: Gander Lake (west half), Newfoundland. Geological Survey of Canada, Map 1195A.

Andrews, K.
1980: Mineral occurrence map, Botwood, Newfoundland. Newfoundland Department of Mines and Energy, Mineral Development Division, Map 80-4.

Blackwood, R.F.
1977: Geology of the east half of the Gambo (2D/16) map area and the northwest portion of the St. Brendan's (2C/13) map area, Newfoundland. Newfoundland Department of Mines and Energy, Mineral Development Division, Report 77-5, 20 pages.

1978: Northeastern Gander Zone, Newfoundland. *In* Report of Activities for 1977. Newfoundland Department of Mines and Energy, Mineral Development Division, Report 78-1, pages 72-79.

1979a: Geology of the Gander River area. *In* Report of Activities for 1978. Newfoundland Department of Mines and Energy, Mineral Development Division, Report 79-1, pages, 38-42.

1979b: Gander River area, Newfoundland. Newfoundland Department of Mines and Energy, Mineral Development Division, Map 7929 (geological and descriptive notes).

1980: Geology of the Gander (west) area (2D/15), Newfoundland. *In* Current Research, Newfoundland Department of Mines and Energy, Mineral Development Division, Report 80-1, pages 53-61.

1981a: Geology of the West Gander River area, Newfoundland. *In* Current Research, Newfoundland Department of Mines and Energy, Mineral Development Division, Report 81-1, pages 50-56.

1981b: Mineral Occurrence Map, Wesleyville, Newfoundland. Newfoundland Department of Mines and Energy, Mineral Development Division, Map 84-23.

1982: Geology of the Gander Lake (2D/15) and Gander River (2E/2) area. Newfoundland Department of Mines and Energy, Mineral Development Division, Report 82-4, 56 pages.

Blackwood, R.F., Colman-Sadd, S.P. and O'Brien, S.
1983: Mineral Occurrence Map, Gander Lake, Newfoundland. Newfoundland Department of Mines and Energy, Mineral Development Division, Map 84-45.

Bradley, D.A.
1962: Gisborne Lake and Terrenceville map areas, Newfoundland. Geological Survey of Canada, Memoir 321.

Butler, A.J. and Davenport, P.H.
1979a: Lake sediment geochemical surveys of the Fortune-Trinity Bay area, Newfoundland. Newfoundland Department of Mines and Energy, Mineral Development Division, Open File Nfld. 1002.

1979b: Fluorine distribution in lake sediments, Fortune-Trinity Bay, Newfoundland. Newfoundland Department of Mines and Energy, Mineral Development Division, Open File Nfld. 966.

1981: Geochemical lake sediment survey, northeastern Newfoundland. Newfoundland Department of Mines and Energy, Mineral Development Division, Open Files 2D (114) and 2E (409).

Butler, A.J., Miller, H.G. and Vanderveer, D.G.
1984: Geoscience studies in the Weir's Pond area northeast of Gander, Newfoundland. *In* Current Research. Newfoundland Department of Mines and Energy, Mineral Development Division, Report 84-1, pages 271-278.

Cochrane, N.A. and Wright, J.A.
1977: Geomagnetic sounding near the northern termination of the Appalachian system. Canadian Journal of Earth Sciences, Volume 14, pages 2858-2864.

Dickson, W.L.
1983: Geology, geochemistry and mineral potential of the Ackley Granite and parts of the North West Brook and Eastern Meelpaeg Complexes, southeast Newfoundland. (Parts of Map Areas 1M/10, 11, 14, 15, 16; 2D/1, 2, 3 and 7) Newfoundland Department of Mines and Energy, Mineral Development Division, Report 83-6, 129 pages.

Haworth, R.T.
1977: The continental crust northeast of Newfoundland and its ancestral relationship to the Charlie Fracture Zone. Nature, Volume 266, pages 246-249.

1981: Geophysical expression of the Appalachian–Caledonide structures on the continental margins of the North Atlantic. *In* Geology of the North Atlantic Borderlands. *Edited by* J. Wm. Kerr and A.J. Ferguson. Canadian Society of Petroleum Geologists, Memoir 7, pages 429-446.

Haworth, R.T. and Jacobi, R.D.
1983: Geophysical correlation between the geological zonation of Newfoundland and the British Isles. Geological Society of America, Memoir 158, pages 25-32.

Haworth, R.T. and Lefort, J.P.
1979: Geophysical evidence for the extent of the Avalon Zone in Atlantic Canada. Canadian Journal of Earth Sciences, Volume 16, pages 552-567.

Haworth, R.T. and Miller, H.G.
1982: The structure of Paleozoic oceanic rocks beneath Notre Dame Bay, Newfoundland. *In* Major Structural Zones and Faults of the Northern Appalachians. *Edited by* P. St. Julien and J. Beland. Geological Association of Canada, Special Paper 24, pages 149-173.

Hays, W.L. and Winkler, R.
1970: Statistics: Probability, Inferences, and Decision. Volume II. Holt, Reinhart, and Winston, New York, pages 1-21.

Henderson, Roland G. and Zeitz, Isidore
1967: The computation of second vertical derivatives of geomagnetic fields. *In* Mining Geophysics, Vol. II. Society of Exploration Geophysicists, pages 606-614.

Jacobi, R.D. and Kristoffersen, Y.
1976: Geophysical and geological trends on the continental shelf off northeastern Newfoundland. Canadian Journal of Earth Sciences, Volume 13, pages 1030-1051.

1981: Transatlantic correlations of geophysical anomalies on Newfoundland, British Isles, France, and adjacent continental shelves. *In* Geology of the North Atlantic Borderlands. *Edited by* J. Wm. Kerr and A.J. Ferguson. Canadian Society of Petroleum Geologists, Memoir 7, pages 197-232.

Jayasinghe, N.P.
1978: Geology of the Wesleyville (2F/4) and the Musgrave Harbour East (2F/5) map areas, Newfoundland. Newfoundland Department of Mines and Energy, Mineral Development Division, Report 78-8, 11 pages.

Jenness, S.E.
1963a: Terra Nova and Bonavista map areas, Newfoundland. Geological Survey of Canada, Memoir 327.

1963b: Geology of the Gander River ultrabasic belt, Newfoundland. Geological Survey of Canada, Report 11.

Keen, C.E., Keen, M.J., Nichols, B., Reid, I., Stockmal, G.S., Colman-Sadd, S.P., O'Brien, S.J., Miller, H.G., Quinlan, G., Williams, H., and Wright, J.A.
1986: Deep seismic reflection profile across the northern Appalachians. Geology, Volume 14, pages 141-145.

Kennedy, M.J. and McGonigal, M.H.
1972: The Gander Lake and Davidsville Groups of northeastern Newfoundland. Canadian Journal of Earth Sciences, Volume 14, pages 488-495.

Leaton, B.R. and Barraclough, D.R.
1971: Grid values for the IGRF 1965.0. International Association of Geomagnetism and Aeronomy, Bulletin 29, 104 pages.

Miller, H.G.
1976: A magnetic model for the Budgell Harbour Stock, Newfoundland. Canadian Journal of Earth Sciences, Volume 13, pages 231-236.

1977: Gravity zoning in Newfoundland. Tectonophysics, Volume 38, pages 317-326.

1983: Gravity surveys. *In* Preliminary Current Research Reports. Newfoundland Department of Mines and Energy, Mineral Development Division, pages 93-95.

1985: Indian Bay Pond area Bouguer gravity anomalies. Mineral Development Division, Newfoundland Department of Mines and Energy, Open File Nfld. 1486.

1986: Gravity surveys in insular Newfoundland, 1985. *In* Current Research. Newfoundland Department of Mines and Energy, Mineral Development Division, Report 86-1, pages 251-256.

Miller, H.G., Goodacre, A.K., Cooper, R.V. and Halliday, D.
1985: Offshore extensions of the Avalon Zone of Newfoundland. Canadian Journal of Earth Sciences, Volume 22, pages 1163-1170.

Miller, H.G. and Weir, H.C.
1982: The northwest portion of the Gander Zone–a geophysical interpretation. Canadian Journal of Earth Sciences, Volume 19, pages 1371-1381.

Mitchelmore, L.
1985: Re-interpretation of the refraction data from Notre Dame Bay, Newfoundland. Unpublished B.Sc. thesis, Memorial University of Newfoundland, 50 pages.

Morelli, C., Gantar, C., Honkasalo, T., McConnell, R.K., Szabo, B., Tanner, J.G., Uotila, U. and Whalen, C.T.
1971: The international standardization gravity net 1971 (IGSN71). International Association of Geodesy and Geophysics, Special Publication No. 4, 194 pages.

Nagy, D.
1967: The gravitational effect of a right-rectangular prism. Geophysics, Volume 31, pages 362-372.

O'Brien, S.J., Nunn, G.A.G., Dickson, W.L. and Tuach, J.
1984: Geology of the Terrenceville (1M/10) and Gisborne Lake (1M/15) map areas, southeast Newfoundland. Newfoundland Department of Mines and Energy, Mineral Development Division, Report 84-4, 54 pages.

O'Neill, P.
1987: Geology of the west half of the Weir's Pond (2E/1) map area. *In* Current Research. Newfoundland Department of Mines and Energy, Mineral Development Division, Report 87-1, pages 271-282.

Pajari, G.E. and Currie, K.L.
1978: The Gander and Davidsville Groups of northeastern Newfoundland: a re-examination. Canadian Journal of Earth Sciences, Volume 15, pages 708-714.

Pajari, G.E., Pickerill, R.K. and Currie, K.L.
1979: The nature, origin, and significance of the Carmanville ophiolitic mélange, northeastern Newfoundland. Canadian Journal of Earth Sciences, Volume 16, pages 1439-1451.

Pal, B.K.
1982: Geomagnetic induction studies in eastern Newfoundland. Unpublished M.Sc. thesis, Memorial University of Newfoundland, 145 pages.

Peavy, S.T.
1985: A gravity and magnetic interpretation of the Bay St. George Carboniferous Sub-basin in western Newfoundland. Unpublished M.Sc. thesis, Memorial University of Newfoundland, 145 pages.

Rasmusen, R. and Pederson, L.B.
1979: End correction in potential field modeling. Geophysical Prospecting, Volume 27, pages 749-760.

Sampson, R.J.
1978: Surface II graphics system, Revision 1. Kansas Geological Survey, 239 pages.

Strong, D.F., Dickson, W.L., O'Driscoll, C.F. and Kean, B.F.
1974: Geochemistry of eastern Newfoundland granitoid rocks. Newfoundland Department of Mines and Energy, Mineral Development Division, Report 74-3, 140 pages.

Tuach, J.
1984: Metallogenic studies of granite associated mineralization in the Ackley Granite and Cross Hills Plutonic Complex, Fortune Bay area, Newfoundland. *In* Current Research. Newfoundland Department of Mines and Energy, Mineral Development Division, Report 84-1, pages 245-253.

1987: The Ackley high-silica magmatic/metallogenic system and associated posttectonic granites, southeast Newfoundland. Unpublished Ph.D. thesis, Memorial University of Newfoundland, 455 pages.

Tuach, J., Davenport, P.H., Dickson, W.L. and Strong, D.F
1986: Geochemical trends in the Ackley Granite, southeast Newfoundland: their relevance to magmatic-metallogenic processes in high silica granitoid systems. Canadian Journal of Earth Sciences, Volume 23, pages 747-765.

Tuach, J., Kerrich, R., Willmore, L.M. and Strong, D.F.
1987: Variations in oxygen isotope related to source terranes and to hydrothermal regimes in the Ackley Granite. *In* 'Granite-Related Mineral Deposits'. Extended Abstracts, R.P. Taylor and D.F. Strong *(Editors)*. Canadian Institute of Mining and Metallurgy, Halifax, pages 285-189.

Weaver, D.F.
1967: A geological interpretation of the Bouguer anomaly field of Newfoundland. Publication of the Dominion Observatory, Ottawa, Volume XXXV, Number 5, pages 223-251.

1968: Preliminary results of the gravity survey of the Island of Newfoundland with maps No. 53, 54, 55, 56 and 57. Earth Physics Branch, Energy, Mines, and Resources, Ottawa.

Weir, H.C.
1971: A gravity profile across Newfoundland. Unpublished M.Sc thesis, Memorial University of Newfoundland, 164 pages.

Whalen, J.B.
1976: Geology and geochemistry of the molybdenite showings of the Ackley Granite, Fortune Bay, Newfoundland. Unpublished M.Sc. thesis, Memorial University of Newfoundland, 276 pages.

Whitten, E.H.T.
1971: Orthogonal polynomial contoured trend surface maps for irregularly spaced data. Computer Applications, Volume 1, pages 171-192.

Williams, H.
1971: Geology of the Belloram map area (1M/11), Newfoundland. Geological Survey of Canada, Map 70-65.

Williams, H. and Hatcher, R.D.
1983: Appalachian suspect terranes. Geological Society of America, Memoir 158, pages 33-54.

Wonderley, P.F. and Neuman, R.B.
1984: The Indian Bay Formation: fossiliferous Early Ordovician volcanogenic rocks in the northern Gander Terrane, Newfoundland, and their regional significance. Canadian Journal of Earth Sciences, Volume 21, pages 525-532.

APPENDIX 1

GRAVITY DATA ACQUISITION AND REDUCTION

The gravity data acquisition and reduction followed the survey and reduction procedure used by the Gravity Division of the Earth Physics Branch, federal Department of Energy, Mines and Resources. First, the gravity reading R_{B1}, at a base tied to, or part of, the Canadian Gravity Network was obtained. Then the gravity readings at the successive stations on the traverse, Rs, were taken and finally a loop closing reading, R_{B2}, at the original base, or at another base was obtained. These data were used to determine the difference in observed g at a station as follows:

$g_{OBS} = g_{BASE} + k_G$ [mGal equivalent to R_s − (mGal equivalent of R_{B2} + drift correction)]

Drift correction = $(t_s - t_{RB1})$*(mGal equivalent of R_{B2} − mGal equivalent of R_{B1})/$(t_{B2} - t_{B1})$

The theoretical gravity at a station location was determined using the 1967 International Gravity Formula

$$g_{THEOR} = 978031.85\ (1 + 0.00530238\ \sin^2\theta - 0.00000585\ \sin^2 2\theta)$$

Then, using this and the expression for the observed gravity, the Bouguer anomaly at a station is calculated assuming a crustal density of 2.67 g cm^{-3} as

$$\Delta g_B = g_{OBS} - g_{THEOR} + \frac{2g_o h}{R_{eq}} - 2\pi\gamma\varrho_c h$$

In operational terms these reduce to

$$\Delta g_B = g_{OBS} - g_{THEOR} + 0.06\ h \quad \text{mGal, when h in feet}$$

or $$\Delta g_B = g_{OBS} - g_{THEOR} + 0.1976\ h \quad \text{mGal, when h in metres}$$

The data for the Canadian Gravity Network bases used are presented in Table A1.1.

Table A1.1 Gravity Base Data

EPB Base Number	Location	Absolute G (mGal)	Elevation (masl)
9211-77	Terrenceville	980857.71	4.00
9218-77	Milltown	980873.83	2.00
9493-76	Northwest Gander Bridge	980919.39	110.00
9216-77	Wesleyville	980988.40	4.00
9217-77	Carmanville	981038.38	5.00
9211-85	Trinity, Bonavista Bay	980977.34	5.76
9212-85	Woods Road	980965.59	58.60
9015-83	Gander	980940.00	143.00

Altimetry Data Acquisition and Reduction

The barometric elevation data acquisition and reduction follows the same basic procedure as that for gravity employing a base station at which an altimeter is kept and read every 5 minutes and two roving altimeters which are read at each station. Dry and wet bulb sling psychrometer temperature readings are recorded every 5 minutes at base and at each station on the traverse.

The base and two roving altimeters are read together at the beginning and end of each traverse to establish both the offset and the offset drift between the base instrument and the roving instrument. The elevation difference between the station and base is corrected for air mass effects using a table of constants furnished by the instrument maker. The elevation of a station is then given by

$$h = e_B + k(T,H)*(B_s-(B_B+DOC))$$

In the above equations the following variables are used

g_{OBS}= observed absolute value of gravity in mGal

g_{BASE}= absolute gravity at base from EPB information in mGal

g_{THEOR}= theoretical value of absolute g in mGal at station location at mean sea level

Δg_B= Bouguer anomaly at station

k_G= instrument constant for meter used

R_S= reading of gravity meter at station

R_{B1}, R_{B2}= reading of gravity meter at base at beginning and end of traverse

mGal equivalent = reading corrected to mGal using meter calibration table

t_s, t_{B1}, t_{B2}= time of reading R_s, R_{B1}, R_{B2} in GMT

θ= latitude of station

h = elevation of station relative to mean sea level

g_o = absolute g at equator at mean sea level

R_{eq}= equatorial radius of the earth

γ= Universal gravitational constant

ϱ_c= mean crustal density, normally 2.67 g cm^{-3}

e_B= elevation of altimetery base

k(T,H) = correction factor as function of average temperature and relative humidity of air mass between station and base

B_s= reading on altimeter at station

B_B= reading on altimeter read at base at same time as reading B_s; this reading is interpolated from 5 minute readings at base

DOC = drift and offset correction applied to B_B to get reading instrument used for B_s would have if at base at time t_o

$$= [B_s(t_1)-B_B(t_1)] + \frac{[(B_s(t_2)-B_B(t_2))-(B_s(t_1)-B_B(t_1))]*(t_s-t_1)}{t_2-t_1}$$

APPENDIX 2

MAGNETIC DATA REDUCTION

The data are digitized by superimposing a 0.5 inch x 0.5 inch grid upon the standard GSC 1:63,360 scale aeromagnetic map constructed from data collected along east–west flight lines flown at a nominal elevation of 1000 ft. (300 m). This results in 47 points in the horizontal (east–west) direction and 35 lines in the vertical (north–south) direction. The value of the magnetic total field is read from the map at each of the grid nodes (intersections). If the map is one of the more recent ones flown using a proton precession magnetometer, the data are the absolute values of the total field at the locations. If the map is one of the older ones for which the data were collected using a fluxgate magnetometer, then the data were corrected to the absolute datum using the following expression, which was determined by comparing values along the boundaries on adjoining maps

$$\text{NEWMAG} = 53293 + 0.9902 * \text{OLDMAG}$$

Once the data sets were expressed as absolute total field magnetic data, the IGRF Epoch 1965.0 was removed by interpolation from published data for 2° squares using the interpolation method suggested by Leaton and Barraclough (1971). Let BF1, BF2, BF3, and BF4 be the absolute total field IGRF values at the reference coordinates 48°N 56°W, 48°N 54°W, 50°N 54°W, and 50°N 56°W respectively. Then at any position inside this square, the IGRF total field is determined from

$$\text{AF2} = \text{BF3} + (\text{LONGITUDE} - 54°)*(\text{BF4}-\text{BF3})/(56° - 54°)$$

$$\text{AF1} = \text{BF2} + (\text{LONGITUDE}-54°)*(\text{BF1}-\text{BF2})/(56° - 54°)$$

$$\text{IGRF(LAT,LONG)} = \text{AF1} + (\text{LATITUDE} - 48°)*(\text{AF2} - \text{AF1})/(50° - 48°)$$

Once the IGRF field at the digitized location is determined, the total field anomaly at that location is determined from

$$\Delta T = \text{digitized value at correct datum} - \text{IGRF (Latitude, Longitude)}$$

This results in a grid of 47 x 35 points at 0.805-km spacing for each 1:36,630 map sheet. Since the gravity data were collected with a station spacing of 2.5 km and a line spacing of 10 km, in order to examine features on the magnetic map having wavelengths similar to those on the gravity map, filtering must be employed. A 25-point averaging filter was used. Using this scheme, the ΔT value at location I, J is replaced by the average of the value at I, J plus the values at the 24 surrounding points. The filter is then moved to the location (I+5, J) and the next average ΔT calculated. This procedure results in a grid of spacing 5 times the original spacing, i.e., 4.25 km. Such a filtering procedure smooths out variations caused by short wavelength features and produces a map having similar wavelengths to the gravity map.

The average ΔT value is given by

$$\begin{aligned}\text{T(I,J)} = 0.04* (&\text{T(I, J)} + \text{T(I+1, J)} + \text{T(I-1, J)} + \text{T(I, J+1)} + \text{T(I, J-1)} + \text{T(I+2, J)} + \text{T(I-2, J)} + \text{T(I, J+2)} + \text{T(I, J-2)} \\ &+ \text{T(I+1, J+1)} + \text{T(I-1, J+1)} + \text{T(I+1, J-1)} + \text{T(I-1, J-1)} + \text{T(I+2, J+2)} + \text{T(I-2, J+2)} + \text{T(I+2, J-2)} \\ &+ \text{T(I-2, J-2)} + \text{T(I-2, J-1)} + \text{T(I-1, J-2)} + \text{T(I+1, J-2)} + \text{T(I+2, J-1)} + \text{T(I+2, J+1)} + \text{T(I-2, J+1)} \\ &+ \text{T(I+1, J+2)} + \text{T(I-1, J+2)})\end{aligned}$$

This averaged ΔT can then be used to calculate the second vertical derivative (Henderson and Zeitz, 1967) of the magnetic map. It fulfills the requirement that the map first be filtered to eliminate near surface effects. The second derivative map was calculated by interpolating the data from the averaging procedure onto a regular 4-km grid using the SURFɯ package and then using the filter option to apply the second derivative filter, the equation for which is given by

$$\begin{aligned}\Delta\text{T2(I, J)} = 0.375* \Delta\text{T(I, J)} - 0.125* &(\Delta\text{T(I+1, J)} + \Delta\text{T(I-1, J)} + \Delta\text{T(I, J+1)} + \Delta\text{T(I, J-1)}) + 0.0313* (\Delta\text{T(I+1, J+1)} \\ &+ \Delta\text{T(I-1, J+1)} + \Delta\text{T(I+1, J-1)} + \Delta\text{T(I-1, J-1)})\end{aligned}$$

which can also be expressed as

$$\Delta\text{T2 (I, J)} = \frac{1}{\Delta^2}[6\Delta\bar{\text{T}}\text{(I, J)} - 8\Delta\bar{\text{T}}\text{(1)} + 2\Delta\bar{\text{T}}(\sqrt{2})] \text{ where } \Delta = 4 \text{ km}$$

where $\Delta\bar{T}(1)$ is the average of the ΔT values 1 unit from (I, J)

and $\Delta\bar{T}(\sqrt{2})$ is the average of the ΔT values 2 units from (I, J).

APPENDIX 3

3-D GRAVITY INVERSION

The objective of gravity inversion is to use the observed gravity data G(x,y,z=0) to directly determine the subsurface structure of the area. To do this the spatial density distribution D(x,y,z) must be known or inferred. In theory,

$$G(x,y,z=0) = \int_{VOL} \frac{D(x,y,z)\ Z\ dxdydz}{[(x-x_o)^2 + (y-y_o)^2 + z)]^{3/2}} \qquad \text{A3-1}$$

The method used in the present study employs a series of right rectangular prisms for which the gravity effect at any location can be rapidly computed (Nagy, 1967). First, both the available gravity and density data were transformed into a new rectangular coordinate system based upon the gravity survey layout. Then, the SURFII package was used to interpolate the existing gravity and density data onto a regular 5-km x 5-km grid. This resulted in 12 lines of data each line having 14 data points. Comparison of the interpolated gravity data with the original data at the same location suggests that the interpolation procedure was an accurate one.

These data were then used to determine the initial thickness of a 5 km x 5 km x T(x,y) right rectangular block to be placed at each grid location to start the gravity computation. The following method was used for computing the initial thickness of the block.

A series of computations using Nagy's 3-D prism program (Nagy, personal communication, 1985) reveals that the gravity effect at the centre of the top surface of a 5 km x 5 km x T right rectangular prism of constant density contrast D can be approximated by the expression

$$\Delta g = 103.4\ D(x,y)\ [1-\exp(-T(x,y)/2.5)] \qquad \text{A3-2}$$

Inverting this one can determine the thickness T of a 5 x 5 x T right rectangular prism needed to produce an anomaly g. But at any location on the survey the anomaly observed is due not only to the gravity effect of the material immediately beneath the location but also to the effect of the material in surrounding prisms. By calculating the gravity effect at the centre of the top surface of a 5 x 5 x T km³ prism and also calculating its effect at 48 surrounding points stepped out successively by 5 km in each of the x and y directions it can be concluded using reciprocity arguments that the total gravity effect at location P(x,y) equals the sum of the effects of prisms located at P(x n x, y m y) where x = y = 5 km, m,n = 0,1,2,3. Summing up these effects for a prism of constant thickness T, one determines that the ratio of the anomaly at P due to the prism immediately beneath it to the sum of the anomalies of all 49 prisms having the same thickness ranges from 0.84 to 0.26 for prisms ranging from 1 to 15 km thick. The mean is approximately 0.5.

Practically, this means that approximately 0.5 of the observed gravity anomaly can be ascribed to the effect of the prism immediately beneath the observation point and the remainder is due to the effects of surrounding prisms. Thus the initial thickness of the prism centred on the observation point can be determined from

$$0.5\ G\ (x,y) = 103.4\ D(x,y)\ [1-\exp(-T(x,y)/2.5)] \qquad \text{A3-3}$$

Once the initial thickness of each prism is determined from this expression, the gravity effect at each grid point is computed as the sum of the gravity effect of the prism immediately beneath the grid point and the gravity effect of each of the surrounding 48 prisms. This limit was chosen after considering the size of the gravity effect of the outer prisms of the 49-prism grid discussed above. This calculated gravity effect was then compared with the observed gravity at each grid location to determine the adjustment to the thickness at that point needed to bring the observed and calculated gravity closer together. The new thickness is then given by

$$T_{i+1} + 1(x,y) = T_i(x,y) + 2\left[\frac{\Delta g_{OBS}(x,y) - \Delta g_{CALC}(x,y)}{41.9\ D(x,y)}\right] \qquad \text{A3-4}$$

The adjustment to the thickness

$$\Delta T = 2\left[\frac{\Delta g_{OBS}(x,y) - \Delta g_{CALC}(x,y)}{41.9\ D(x,y)}\right] \qquad \text{A3-5}$$

is twice the iteration one calculates using an infinite horizontal slab effect. This was chosen since the prism has a more concentrated horizontal mass distribution, therefore, to achieve the same change in gravity, the change in thickness must be greater than for the horizontal slab. At first, the derivative of the inverse of the expression A3.2 was tried but this resulted in unstable changes in T approaching or exceeding the value of T itself, so the simpler approach was used as it led to stabler conversion.

After the new T(x,y) values are computed the T(x,y) matrix is smoothed using

$$T(I,J) = 0.7\ T(I,J) + 0.04375\ *(T(I, J+1) + T(I, J-1) + T(I+1, J) + T(I-1, J)) + 0.03125\ *(T(I+1, J+1) + T(I-1, J+1) + T(I+1, J-1) + T(I-1, J-1)) \qquad \text{A3-6}$$

This process distributes some of the changes in thickness to the adjoining prisms, leading to a smoother distribution of thickness and a more rapid convergence.

The iteration process is then continued and the calculated g determined for the new thickness distribution. The average difference between the observed and calculated g_B is determined along with the standard deviation of the differences. If this is less than 1 mGal the iteration process is stopped, if not, a new iteration to thickness is computed and the procedure is continued until a fixed number of iterations is completed. By examining the statistics of each iteration the one having the minimum variance can be chosen as the best model.

The procedure converges rapidly with a minimum variance model being reached after 3 iterations in the variable density case and after 8 iterations in the constant density case.

APPENDIX 4

SPATIAL CROSS-CORRELATION TECHNIQUES

In this appendix, the spatial cross-correlation techniques used in examining the degree of cross correlation between two data sets not necessarily having the same geographic distribution of sampling locations is presented.

If two data sets, A and B are available for the same general geographic area and the sampling locations do not in general coincide, then one cannot determine quantitatively the degree of correlation using a measure such as the Pearson product moment correlation coefficient. But if the two data sets are each reasonably well distributed over the same general geographic area an interpolation method may be used to interpolate each data set onto the same regular grid. Such a package is available in the SURFII Graphics package (Sampson, 1978). The choice of the grid spacing is a decision to be made by the user. In correlating the gravity and physical property data or the gravity and geochemical data, a 5-km grid was used as this was most compatible with the gravity data, which consisted of 254 data points whereas the other data sets contained 656 data points.

Once this interpolation has been undertaken it is a simple matter to compute the Pearson product moment correlation coefficient r_{xy} from the two interpolated data sets A and B having N values at each of the k = 1, ... N common interpolated locations.

$$R_{xy} = \sum_{k=1}^{N} \frac{[A(x,y)-a]\,[B(x,y)-b]}{NS_aS_b}$$

$$a = \frac{1}{N}\sum_{k=1}^{N} A(x,y) \qquad b = \frac{1}{N}\sum_{k=1}^{N} B(x,y)$$

$$S_a = \frac{1}{N}\sum_{k=1}^{N} (A(x,y)-a)^2 \qquad S_b = \frac{1}{N}\sum_{k=1}^{N} (B(x,y)-b)^2$$

This is effectively the ensemble average correlation coefficient for the two interpolated data sets. It can be written as

$$R_{xy} = \frac{1}{N}\sum_{k=1}^{N} \frac{[A(x,y)-a]}{S_a} \quad \frac{[B(x,y)-b]}{S_b}$$

$$= \frac{1}{N}\ r_{ij}$$

$$\text{where } r_{ij} = \frac{[A(x,y)-a]}{S_a} \quad \frac{[B(x,y)-b]}{S_b}$$

$$= \text{standard Z score of A(x,y)} \ * \ \text{standard Z score of B(x,y)}$$

This r_{ij} is the value of the correlation coefficient between the two variables A and B at the location ij. It is obvious from the above definition of r_{ij} that it is the product of the Z score of the A variable at some location multiplied by the Z score of the B variable at that same location. The standard correlation coefficient, r_{xy}, is seen to be simply the ensemble mean of the r_{ij}'s. By plotting a map of r_{ij}, areas of exceptional correlation between the two data sets may be examined and geographic trends in the cross correlation examined quantitatively.

The r_{xy} value indicates the overall correlation coefficient for the data sets and can be tested for significance using standard statistical methods (Hays and Winkler, 1970).

APPENDIX 5

REDUCED BOUGUER ANOMALY DATA

Table A5.1. Data Listing for 72 Gravity Stations, Ackley Area, June 1986 Survey

Station	Easting	Northing	Elevation	Bouguer
8601.	667.300	5296.900	552.	-8.6
8602.	669.300	5298.875	727.	-6.4
8603.	671.225	5300.300	643.	-9.5
8604.	673.325	5301.575	533.	-10.3
8605.	675.900	5303.300	584.	-10.8
8606.	670.775	5310.450	698.	-6.9
8607.	668.225	5308.825	711.	-2.3
8608.	666.300	5307.400	691.	-3.2
8609.	664.175	5305.950	605.	-6.1
8610.	661.675	5305.200	565.	-8.4
8611.	659.700	5303.175	626.	-9.3
8612.	657.600	5301.875	604.	-11.1
8613.	655.700	5300.200	618.	-12.1
8614.	653.825	5298.375	44.	-14.5
8615.	651.175	5297.325	688.	-13.8
8616.	648.800	5295.625	794.	-14.4
8617.	646.950	5294.825	750.	-14.6
8618.	644.425	5293.925	826.	-14.8
8619.	642.625	5292.200	643.	-14.9
8620.	649.650	5290.625	708.	-15.7
8621.	638.625	5289.275	737.	-17.1
8622.	636.500	5287.750	117	-18.9
8623.	634.500	5286.400	583.	-17.4
8624.	632.500	5284.750	624.	-13.9
8625.	630.250	5283.650	581.	-10.4
8626.	628.100	5281.750	762.	-2.2
8627.	625.850	5279.750	4.	6.4
8628.	619.225	5288.375	924.	3.0
8629.	622.575	5290.325	502.	-0.6
8630.	625.150	5290.850	366.	-1.1
8631.	626.900	5292.900	579.	1.3
8632.	628.900	5294.375	713.	-2.3
8633.	630.925	5296.050	780.	-10.3
8634.	632.950	5296.900	671.	-13.3
8635.	635.100	5299.150	649.	-13.3
8636.	662.550	5317.950	648.	-6.4
8637.	659.850	5316.625	591.	-8.8
8638.	657.875	5314.825	556.	-9.3
8639.	656.300	5313.375	530.	-10.3
8640.	653.325	5311.850	513.	-11.0
8641.	651.700	5310.300	438.	-11.4
8642.	648.950	5309.375	592.	-12.2
8643.	646.650	5307.875	627.	-12.3
8644.	645.450	5305.850	654.	-12.9
8645.	643.300	5304.765	648.	-12.8
8646.	641.500	5302.900	706.	-12.3
8647.	640.100	5302.300	800.	-13.3
8648.	637.250	5300.500	743.	-14.0
8649.	633.950	5280.300	311.	-6.2
8650.	637.700	5278.325	465.	-6.6

Table A5.1. *Continued*

Station	Easting	Northing	Elevation	Bouguer
8651.	662.750	5293.900	560.	-11.2
8652.	656.225	5290.250	494.	-15.2
8653.	659.375	5285.700	829.	-8.4
8654.	657.650	5288.000	732.	-13.5
8655.	653.975	5288.875	442.	-16.4
8656.	651.325	5288.350	361.	-17.9
8657.	655.875	5286.875	518.	-15.0
8658.	653.200	5285.350	655.	-12.0
8659.	656.900	5284.200	1214.	-9.7
8660.	654.675	5283.200	792.	-4.5
8661.	660.700	5284.000	905.	-3.7
8662.	658.550	5282.575	794.	-2.2
8663.	656.100	5281.300	946.	-3.8
8664.	650.925	5274.950	5.	-1.8
8665.	646.700	5273.350	5.	-7.6
8666.	644.425	5276.000	317.	-15.8
8667.	648.525	5278.775	882.	-6.7
8668.	647.750	5284.950	6.	-14.4
8669.	645.775	5282.950	586.	-9.9
8670.	643.800	5281.875	751.	-13.3
8671.	641.500	5280.100	501.	-14.0
8672.	641.325	5273.775	13.	-13.4